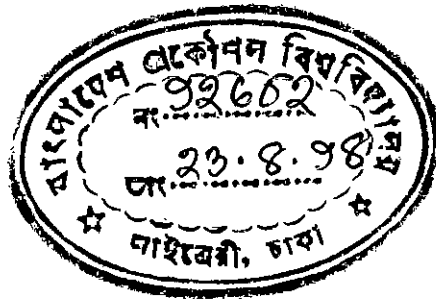


**STUDY OF DISPERSION COMPENSATION
SCHEMES IN A POINT TO POINT TRANSMISSION
WITH CASCADED OPTICAL AMPLIFIER**

A thesis submitted to the department of
Electrical and Electronic Engineering BUET, Dhaka,
in partial fulfillment of the
requirements for the degree of
Master of Science in Engineering
(Electrical and Electronic)



MD. HASANUZZAMAN

August 1998



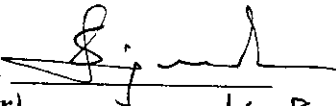
DEDICATED TO MY PARENTS

APPROVAL


This thesis titled “study of dispersion compensation schemes in a point to point transmission with cascaded optical amplifier” submitted by MD. HASANUZZAMAN, Roll No. 9406208P, session 1993-94-95 to the Department of Electrical and Electronic Engineering, BUET has been accepted as satisfactory for the partial fulfillment of the requirements for the degree of **Master of Science in Engineering (Electrical and Electronic)**

Board of Examiners

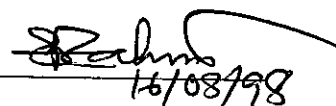
1. **Dr. S. P. Majumder**
Professor
Department of EEE
BUET, Dhaka-1000.

Chairman 
(Supervisor) 16.8.98

2. **Dr. Enamul Basher**
Professor and Head
Department of EEE
BUET, Dhaka-1000.

Member 
(Ex-officio) 16.8.98

3. **Dr. Md. Saifur Rahman**
Professor
Department of EEE
BUET, Dhaka-1000.

Member 
16/08/98

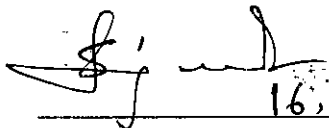
4. **Dr. M. Kaykobad**
Professor and Head
Department of CSE
BUET, Dhaka-1000.

Member 
(External)

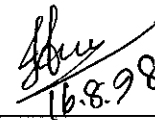
DECLARATION

I hereby declare that this work has not been submitted elsewhere for the award of any degree or diploma.

Countersigned


16.8.98

(Dr. S. P. Majumder)


16.8.98

(Md. Hasanuzzaman)

CONTENTS

ACKNOWLEDGMENTS	vii
ABSTRACT	viii
LIST OF FIGURES	ix
LIST OF PRINCIPAL SYMBOLS.	xiv
LIST OF ABBREVIATIONS.	xvi
CHAPTER-1 INTRODUCTION	1
1.1 Prologue	1
1.2 Limitations of Optical Fibre Communication	6
1.3 Review of previous works	7
1.4 Objective of the present study.	9
1.5 Brief introduction to this Thesis	10
CHAPTER-2 PERFORMANCE ANALYSIS OF A POINT TO POINT OPTICAL CPFSK TRANSMISSION SYSTEM	11
2.1 Overview	11
2.2 System Model	12
2.3 The Receiver Model.	14
2.3.1 MZI characteristics.	14

2.4	Theoretical Analysis for Optical Direct detection CPFSK . . .	17
2.4.1	FSK with NRZ data	17
2.4.1.1	Lump compensation	19
2.4.1.2	Even compensation	20
2.4.1.3	The Receiver output signal	21
2.4.1.4	Bit Error Rate Expression	24
2.4.2	Effect of Self Phase Modulation(SPM).	25
2.4.3	CPFSK system with Line Coding	27
CHAPTER-3 RESULTS AND DISCUSSIONS		32
CHAPTER-4 CONCLUSIONS AND SUGGESTIONS FOR . . .		68
FUTURE WORK		
4.1	Conclusions.	68
4.2	Future works	70
REFERENCES.		71

ACKNOWLEDGEMENTS

I would like to express my sincerest and profound gratitude to my honourable supervisor Dr. S. P. Majumder, Professor of the Department of Electrical and Electronic Engineering, BUET, for his consistent but friendly supervision and encouragement throughout the completion of this work. He patiently gave many valuable advices, proper guidance, constructive suggestions and kind cooperation during this research work. I owe him for entire work.

I would like to take the opportunity to express the deepest appreciation to Dr. Enamul Basher, Professor and head of the Department of EEE, BUET, for providing Departmental facilities.

Special thanks to Dr. Saifur Rahman, Professor, Department of EEE, for his cooperation and constant encouragement specially in computer programming related works.

Finally, I would like to thank my parents who inspired me for the completion of the M.Sc. Degree, also to Md. Rafiqul Islam, Md. Faizul Momen and Bikash Chandra sarker for their support, continuous inspiration and constant encouragement towards the completion of this work.

ABSTRACT

A theoretical analysis is carried out to evaluate the efficiency of two different dispersion compensation schemes, viz. lump compensation and even compensation to minimize the effect of group velocity dispersion (GVD) on the performance of an optical CPFSK point to point transmission system using MZI based direct detection receiver. The analysis is extended to line-coded CPFSK system with three line-coding schemes, viz. Alternate mark inversion (AMI), Miller code or Delay modulation (DM) and Manchester code (MC). The analysis is also carried out to find out the impact of SPM with GVD compensation.

The analysis includes the effect of accumulated amplifiers spontaneous emission (ASE) noise, signal-ASE noise, ASE-ASE beat noise, laser phase noise and receiver noise. The statistics of the phase fluctuations due to chromatic dispersion in the presence of filtering effect and laser phase noise are determined analytically and is used to determine the bit error probability of the direct detection FSK receiver. The analysis is first carried out for NRZ data pattern and then extended to line-coded data patterns with three different line-coding schemes, viz. AMI, DM, MC to investigate the effectiveness of the line-coding schemes in presence of dispersion. Following the theoretical analysis, the bit error rate (BER) performance of the optical link is evaluated for NRZ and line-coded data pattern at a bit rate of 10 Gb/s for different system parameters. The power penalty suffered by the system due to the system imperfections mentioned above at $BER=10^{-9}$ is evaluated. The improvement in system performance due to the use of compensation schemes is then determined for NRZ data. Performance degradation due to SPM is also evaluated.

LIST OF FIGURES

- Fig. 1 Generalized block diagram of an optical communication system.
- Fig. 2.1 Block diagram of an optical CPFSK transmission system with lump compensation.
- Fig. 2.2 Block diagram of an optical CPFSK transmission system with even compensation
- Fig. 2.3 Block diagram of a CPFSK direct detection receiver with Mach-Zender Interferometer (MZI) as an optical frequency discriminator (OFD).
- Fig. 2.4 (a) An MZI with large ΔL or narrow wavelength spacing,(b) Transmittance characteristics of an MZI and (c) Differential output of the balanced receiver.
- Fig. 2.5 (a) Tabular and state diagram of Alternate Mark inversion (AMI) line code.
- Fig. 2.5 (b) Tabular and state diagram of Delay Modulation (DM) line code.
- Fig. 2.5 (c) Tabular and state diagram of Manchester Code (MC) .
- Fig. 2.6 Power spectral density of different line codes : NRZ, AMI, DM and MC.
- Fig. 3.1 The bit error rate (BER) performance of a point to point optical direct detection CPFSK link with lump compensation at a bit rate of 10 Gb/s with dispersion coefficient $D_c \& D'_c = 15\text{ps/nm-km}$, fibre length $L=40$ km at an wavelength of 1550 nm and modulation index $h=1$ for several values of compensator length.
- Fig. 3.2 The bit error rate (BER) performance of a point to point optical direct detection CPFSK link with lump compensation at a bit rate of 10 Gb/s with dispersion coefficient $D_c \& D'_c = 15\text{ps/nm-km}$, fibre length $L=60$ km at an wavelength of 1550 nm and modulation index $h=1$ for several values of compensator length.

- Fig. 3.3 The bit error rate (BER) performance of a point to point optical direct detection CPFSK link with lump compensation at a bit rate of 10 Gb/s with dispersion coefficient $D_c \& D'_c = 15\text{ps/nm-km}$, fibre length $L=80$ km at an wavelength of 1550 nm and modulation index $h=1$ for several values of compensator length.
- Fig. 3.4 Plots of penalty in signal power due to fibre chromatic dispersion for a point to point optical CPFSK link without any compensation versus with fibre length L at $\text{BER}=10^{-9}$ and modulation index $h=0.5$ and $h=1$.
- Fig. 3.5 Plots of penalty in signal power due to GVD in a point to point optical CPFSK link with lump compensation at $\text{BER}=10^{-9}$ versus $D'_c L'$ with fibre length $L=40, 60, 80$ km and modulation index $h=1$.
- Fig. 3.6 Plots of penalty in signal power due to GVD in a point to point optical CPFSK link with lump compensation at $\text{BER}=10^{-9}$ versus $D'_c L'$ with fibre length $L=40, 60, 80$ km and modulation index $h=0.5$.
- Fig. 3.7 The bit error rate (BER) performance of a point to point optical link with even compensation for direct detection FSK system at a bit rate of 10 Gb/s with dispersion coefficient $D_c \& D'_c = 15\text{ps/nm-km}$, fibre length $L=100$ km, compensator length in each section $L'_a = 10\text{km}$, modulation index $h=1$ at an wavelength of 1550 nm, for several number of fibre sections N .
- Fig. 3.8 The bit error rate (BER) performance of a point to point optical link with even compensation for direct detection FSK system at a bit rate of 10 Gb/s with dispersion coefficient $D_c \& D'_c = 15\text{ps/nm-km}$ fibre length $L=100$ km, compensator length in each section $L'_a = 20\text{km}$, modulation index $h=1$ at an wavelength of 1550 nm, for several number of fibre sections N .
- Fig. 3.9 The bit error rate (BER) performance of a point to point optical link with even compensation for direct detection FSK system at a bit rate of 10 Gb/s with dispersion coefficient $D_c \& D'_c = 15\text{ps/nm-km}$, fibre length $L=100$ km, compensator length in each section $L'_a = 40\text{km}$, modulation index $h=1$ at an wavelength of 1550 nm, for several number of fibre sections N .

- Fig. 3.10 Plots of penalty in signal power due to GVD in a point to point optical link with even compensation at of $BER=10^{-9}$ versus number of fibre section with fibre length $L=100$ km compensator length in each section $L'_a = 10, 20, 40$ km and modulation index $h=1$.
- Fig. 3.11 Plots of penalty in signal power due to GVD in a point to point optical link with even compensation at of $BER=10^{-9}$ versus number of fibre section with fibre length $L=300$ km compensator length in each section $L'_a = 40, 60, 80$ km and modulation index $h=1$.
- Fig. 3.12 Plots of minimum penalty in signal power of a point to point optical link with even compensation at $BER=10^{-9}$ versus number of fibre section with fibre length $L=100$ km and 300 km and modulation index $h=1$.
- Fig. 3.13 The bit error rate (BER) performance of a point to point optical link with lump compensation in presence of GVD and SPM for direct detection FSK system at a bit rate of 10 Gb/s with dispersion coefficient $D_c \& D'_c = 15$ ps/nm-km, fibre length $L=50$ km, $P_{in}=0$ dBm at an wavelength of 1550 nm and modulation index $h=1$ for several values of compensator length L' .
- Fig. 3.14 The bit error rate (BER) performance of a point to point optical link with lump compensation in presence of GVD and SPM for direct detection FSK system at a bit rate of 10 Gb/s with dispersion coefficient $D_c \& D'_c = 15$ ps/nm-km, fibre length $L=50$ km, $P_{in}=5$ dBm at an wavelength of 1550 nm and modulation index $h=1$ for several values of compensator length L' .
- Fig. 3.15 The bit error rate (BER) performance of a point to point optical link with lump compensation in presence of GVD and SPM for direct detection FSK system at a bit rate of 10 Gb/s with dispersion coefficient $D_c \& D'_c = 15$ ps/nm-km, fibre length $L=50$ km, $P_{in}=8$ dBm at an wavelength of 1550 nm and modulation index $h=1$ for several values of compensator length L' .
- Fig. 3.16 Plots of penalty in signal power due to GVD and SPM in a point to point optical link with lump compensation at of $BER=10^{-9}$ versus compensator length L' with dispersion coefficient $D_c \& D'_c = 15$ ps/nm-km, fibre length $L=50$ km, $P_{in} = 0, 5, 8$ dBm and modulation index $h=1$.

- Fig. 3.17 Plots of penalty in signal power due to GVD and SPM in a point to point optical link with lump compensation at of $BER=10^{-9}$ versus compensator length L' with dispersion coefficient D_c & $D'_c = 15\text{ps/nm-km}$, fibre length $L=50\text{km}$, $P_{in} = 0, 5, 8$ dBm and modulation index $h=0.5$.
- Fig. 3.18 Plots of penalty in signal power due to GVD and SPM in a point to point optical link with lump compensation at of $BER=10^{-9}$ versus fibre input power for fibre length $L=50\text{km}$ and modulation index $h=1$ with compensator length as parameter.
- Fig. 3.19 Plots of penalty in signal power due to GVD and SPM in a point to point optical link with lump compensation at $BER=10^{-9}$ versus fibre input power for fibre length $L=50\text{km}$ and modulation index $h=0.5$ with compensator length as parameter.
- Fig. 3.20 The bit error rate (BER) performance of an optical CPFSK link without any compensation with AMI line coded bit pattern at a bit rate of 10 of Gb/s with fibre chromatic dispersion $D_c=15\text{ps/nm-km}$, modulation index $h=1$ at an wavelength of 1550 nm, with fibre length L as parameter.
- Fig. 3.21 The bit error rate (BER) performance of an optical CPFSK link without any compensation with AMI line coded bit pattern at a bit rate of 10 of Gb/s with fibre chromatic dispersion $D_c=15\text{ps/nm-km}$, modulation index $h=0.5$ at an wavelength of 1550 nm, with fibre length L as parameter.
- Fig. 3.22 Plots of penalty in signal power due to GVD in a point to point optical CPFSK link without any compensation versus fibre length with AMI line coded bit pattern at a bit rate of 10 Gb/s at $BER=10^{-9}$ with modulation index h as parameter.
- Fig. 3.23 The bit error rate (BER) performance of an optical CPFSK link without any compensation with DM line coded bit pattern at a bit rate of 10 of Gb/s with fibre chromatic dispersion $D_c=15\text{ps/nm-km}$, modulation index $h=1$ at an wavelength of 1550 nm, with fibre length L as parameter.
- Fig. 3.24 The bit error rate (BER) performance of an optical CPFSK link without any compensation with AMI line coded bit pattern at a bit rate of 10 of Gb/s with fibre chromatic dispersion $D_c=15\text{ps/nm-km}$, modulation index $h=0.5$ at an wavelength of 1550 nm, with fibre length L as parameter.

Fig. 3.24 The bit error rate (BER) performance of an optical CPFSK link without any compensation with AMI line coded bit pattern at a bit rate of 10 Gb/s with fibre chromatic dispersion $D_c=15\text{ps/nm-km}$, modulation index $h=0.5$ at an wavelength of 1550 nm, with fibre length L as parameter.

Fig. 3.25 Plots of penalty in signal power due to GVD in a point to point optical CPFSK link without any compensation versus fibre length with DM line coded bit pattern at a bit rate of 10 Gb/s at $\text{BER}=10^{-9}$ with modulation index h as parameter.

Fig. 3.26 The bit error rate (BER) performance of an optical CPFSK link without any compensation with MC line coded bit pattern at a bit rate of 10 Gb/s with fibre chromatic dispersion $D_c=15\text{ps/nm-km}$, modulation index $h=1$ at an wavelength of 1550 nm, with fibre length L as parameter.

Fig. 3.27 The bit error rate (BER) performance of an optical CPFSK link without any compensation with MC line coded bit pattern at a bit rate of 10 Gb/s with fibre chromatic dispersion $D_c=15\text{ps/nm-km}$, modulation index $h=0.5$ at an wavelength of 1550 nm, with fibre length L as parameter.

Fig. 3.28 Plots of penalty in signal power due to GVD in a point to point optical CPFSK link without any compensation versus fibre length with MC line coded bit pattern at a bit rate of 10 Gb/s at $\text{BER}=10^{-9}$ with modulation index h as parameter.

Fig. 3.29 Plots of penalty in signal power due to GVD in an optical direct detection CPFSK system with full compensation versus fibre length for different line-coding data pattern at a bit rate of 10 Gb/s at $\text{BER}=10^{-9}$ with modulation index h as parameter.

LIST OF PRINCIPAL SYMBOLS

B_r	Bit rate
σ^2	Noise variance
$n(t)$	Complex additive Gaussian noise
Δf	Frequency deviation of FSK signal
ϕ_n	Phase noise of transmitting laser
ϕ_s	Angle modulation
h	Modulation index
R_d	Photon responsivity
P_s	Input optical signal power
f_c	Optical carrier frequency
$H_f(f)$	Optical fibre transfer function for lump compensation
$H_c(f)$	Compensator transfer function for lump compensation
$H'_f(f)$	Optical fibre transfer function for even compensation
$H'_c(f)$	Compensator transfer function for even compensation
D_c	Fibre dispersion coefficient
D'_c	Compensator dispersion coefficient
L	Fibre length
L'	Compensator length
L_a	Fibre length in each section of even compensation
L'_a	Compensator length in each section of even compensation
λ	Optical wavelength
ν	Frequency of optical carrier

$\Delta\nu$	Normalized linewidth of transmitting laser
τ	Delay occurred due to path difference in MZI
l_1, l_2	Lengths of arms I and II of MZI
T_I, T_{II}	Transmittance of arms I and II of MZI
ΔL	Path difference of MZI
η_{eff}	Effective refractive index of MZI
$I(t)$	Modulating signal
F	Fourier transform
F^{-1}	Inverse Fourier transform
c	Velocity of light
k	Boltzman's constant
$\delta(t)$	Delta function of time
$P(\Delta\theta_n)$	PSD of $\Delta\theta_n$
G_a	ASE factor
N_{sp}	Spontaneous emission factor
$N_{\text{s-sp}}$	Signal spontaneous noise power
$N_{\text{sp-sp}}$	Spontaneous spontaneous noise power
S_{pd}	Photo-detector shot noise
S_{pdi}	Interferometric noise
S_{th}	Receiver thermal noise
$G_{\text{FSK-PN}}(f)$	PSD of the FSK signal corrupted by noise
$G_{\text{FSK}}(f)$	PSD of FSK signal
$G_{\text{PN}}(f)$	PSD of laser phase noise
B	Optical bandwidth
B_e	Electrical bandwidth

LIST OF ABBREVIATIONS

ASK	Amplitude shift keying
APD	Avalanche photo diode
ASE	Accumulated spontaneous emission
BER	Bit error rate
CPFSK	Continuous phase FSK
dBm	Decibel relative to 1 mw
DFB	Distributed feedback
EDFAs	Erbium doped fibre amplifiers
erfc	Complimentary error function
FM	Frequency modulation
FSK	Frequency shift keying
FDM	Frequency division multiplexing
FWM	Four wave mixing
GVD	Group velocity dispersion
IF	Intermediate frequency
IM/DD	Intensity modulation direct detection
ISI	Inter-symbol interference
LASER	Light amplification by stimulated emission of radiation
LD	Laser diode
LED	Light emitting diode
MZI	Mach-Zehnder interferometer
NRZ	Non-return to zero
OOK	On-off keying
OFD	Optical frequency discriminator
OFDM	Optical frequency division multiplexing
OTDM	Optical time division multiplexing

PDF	Probability density function
PIN	Positive intrinsic negative
PSD	Power spectral density
QPSK	Quadrature phase shift keying
SLD	Semiconductor laser diode
SPM	Self phase modulation
SNR	Signal to noise ratio
SONET	Synchronous optical network
WDM	Wavelength division multiplexing

CHAPTER-1

INTRODUCTION



1.1 Prologue

The invention of (LASER) in 1960 and also the invention of Optical fibre by Kao and Hockham in 1965 made enormous developments in Optical fibre communication system. Since then opto-electronics technology has been continuously improving and optical communication has been possible with application in point to point links. The use of optical fibre as communication medium has been continuously growing up during the last two decades. The present trend is such that in the near future optical fibre communications will be the heart of information technology all over the world. The optical fibre communication system has the following advantages by virtue of its characteristics :

- High bandwidth (1 GHz-Km to over 1 THz-Km) ;
- Higher bit rate (100 Mb/s to 10 Gb/s) ;
- Low attenuation (0.1 dB/km to 0.3 dB/km);
- Light weight (smaller in diameter compared to co-axial cable) ;
- Electrical immunity (no RFI, EMI interference) ;
- Security (can not be easily tapped, no cross talk) ;
- Flexibility (easy to install) ;
- Falling cost (less than \$ 100/km of cabled fibre) ;
- Long repeater spacing (more than 100 km) ;

Due to the above features, research activities around the world is encouraged in optical fibre communication and led to have around 50 million kilometers of optical fibre installed world wide [1-2].

During 1965-75 graded index fibre utilizing wavelength of 850-900nm was developed, and using this the information rate in the range of 8-140Mbit/s was achieved. Single mode fibre was developed in 1978 and was utilized in transmission at the wavelength of 1300 nm. The present trend is towards using 1500 nm fibre for long haul system due to the recent developments in long wavelength semiconductor laser diodes (SLDs). By 1980s, these activities had led to the development and worldwide installation of practical and economically feasible optical fibre communication systems that can carry telephone, cable television, data and other telecommunication traffics.

The block diagram of an optical communication system is shown in Fig. 1.

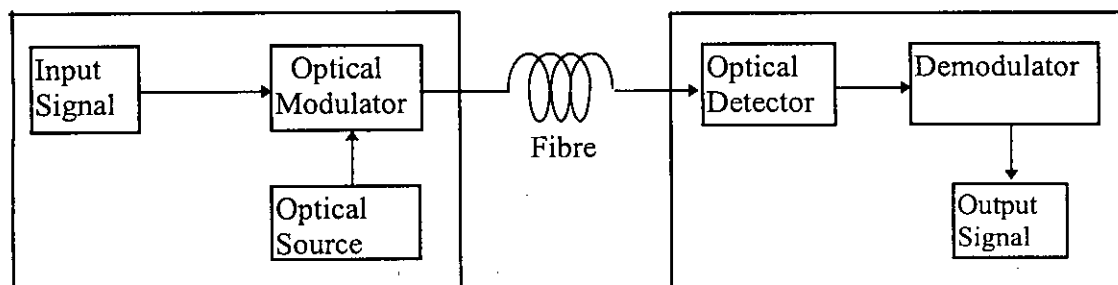


Fig. 1. Generalized block diagram of an optical communication system.

The main components are :

- Optical source ;
- Optical modulator ;
- Optical fibre as transmission waveguide ;
- Optical detector ;
- Demodulator ;

In an optical communication system electrical signals are first converted into optical or light signals by modulating an optical source such as light emitting diode (LED) or laser diode (LD). Then the optical signal is launched into the fibre and is transmitted over a long distance. At the receiving end the optical signal is converted to electrical signal by avalanche photodetector (PD) or PIN photodetector followed by a receiver.

Two conventional light sources are used in optical fibre communication, they are: Light emitting diodes (LEDs) and Laser diodes (LDs). The advantages of LED are (i) less sensitive to retroreflection (ii) possesses no interference problem (iii) less sensitive to temperature variation (iv) high reliability (v) simple electronic excitation and (vi) less costly. But main disadvantages are (i) low coupling efficiency between an LED and a fibre (ii) low modulation bandwidth, typically limited to 100 MHz to 200 MHz (iii) wide spectral width of about 50-100 MHz around 50 nm.

The advantages of LD are (i) high conversion gain i.e. with small bias current relatively high power output (ii) low numerical aperture, as a result, coupling efficiency is high (iii) high modulation bandwidth (GHz) (iv) narrow spectral width (10-50Mhz). The main disadvantages of LD are that it (i) is highly sensitive to temperature variation (ii) produce supplementary to return reflected power (iii) less reliable (iv) more costly. In summary, for short links (< 10 km) LED is suitable, but for medium and long links LD is suitable.

Two types of photodetectors are frequently used in optical fibre communication system i) PIN (Positive-Intrinsic-Negative) photodiode and ii) Avalanche photodiode (APD). For short links Ge PIN is used. For medium links Ge III/V PIN or Ge APD is used and for long links III/V APD is used.

After optical signal has been launched into the fibre, it becomes progressively attenuated and distorted with increasing distance because of scattering, absorption, dispersion in the fibre. At the receiver the attenuated and distorted optical power is detected by the photodiode. The figure of merit for a fibre is the attenuation and distortion which should be minimum, and for a receiver there is a minimum optical power necessary at the desired data rate to attain either a given error probability for a digital system or a specified signal to noise ratio for an analog system.

In optical communication systems, there are two important detection techniques are normally employed i) direct detection ii) coherent detection. In direct detection, a photodetector only responds to changes in the power level (the intensity) of an optical signal, and not to its frequency and phase content. So this is known as intensity modulation (IM). At the receiving end, one then uses direct detection (DD) to convert the optical signal into an electrical signal. The IM/DD systems are simple and relatively less costly, but they suffer from limited sensitivity and do not take full advantage of the tremendous bandwidth capabilities of optical fibres, due to relatively low optical power output of semiconductor laser diode (SLD). Direct detection optical communication systems were found very promising for future deep space applications, inter-satellite links and terrestrial line of sight communications. To increase the data rate throughput of all semiconductor free space optical channels, extensive research for bandwidth, power efficient coding and modulation schemes were carried out in the last decade [3-5].

Coherent light wave communication systems using heterodyne or homodyne are becoming more attractive for long haul transmission and wide band data distribution. Two major advantages that coherent systems offer are (i) improved receiver sensitivity (up to 20 dB) relative to direct detection so that either the bit rate or the repeater spacing can be greatly increased, ii) a high

degree of frequency selectivity on optical wavelength division multiplexing (WDM) system [3]. In coherent optical communication system, information can be impressed on the optical carrier in one of the three ways i) phase shift keying (PSK) ii) frequency shift keying (FSK) iii) amplitude shift keying (ASK). Depending on the specific application various modulation and demodulation formats, similar to those of traditional radio frequency communication, are also employed in coherent lightwave transmission [5-8]. These include binary PSK (BPSK), quadrature PSK (QPSK), orthogonal QPSK (OQPSK), continuous phase FSK (CPFSK), discontinuous phase FSK (DPFSK), binary pulse position modulation (BPPM) etc. Each of the modulation schemes viz. ASK, FSK, DPSK etc. and combinations thereof, with homodyne, heterodyne or diversity receivers has its own merits and demerits and none has emerged as absolutely preferable. However, FSK systems are more promising than ASK or PSK due to several reasons. First, modulation can be easily performed using direct modulation of laser diode (LD) through its injection current [6,7]. FSK is flexible enough to allow generation of either compact spectra, which is advantageous in multichannel WDM or two lobe spectra which allows for receiver envelope detection by properly selecting the modulation index. Further, a laser FM transmitter and a receiver front-end can easily be converted to encompass subcarrier modulation scheme, such as MSK-FM for instance and subcarrier multiplexing.

Actually, the huge transmission capacity of single mode fibers can be exploited efficiently by accessing the fibre bandwidth in the wavelength domain rather than in the time domain [8]. Among WDM systems, dense Wavelength Division multiplexing (in which the channels spacing is a few times the bit rate) allow the possibility of transmitting many channels simultaneously, increasing the transmission capacity. A sharp cut-off filter and a modulation scheme with a compact spectrum are necessary to construct densely spaced multiplexing systems utilizing a direct detection scheme.

1.2 Limitations of Optical Fibre Communications

In spite of several advantages, there are some limitations of optical fibre communication systems due to the following effects [9-24]

- Stimulated Raman Scattering (SRS) ;
- Stimulated Brillouin Scattering (SBS) ;
- Cross-phase Modulation (XPM) ;
- Four wave mixing (FWM) ;
- Chromatic dispersion or Group velocity dispersion (GVD) ;
- Laser phase noise ;
- Self phase noise (SPM) ;
- Optical amplifiers' spontaneous emission (ASE) noise ;

Stimulated Raman Scattering is an interaction between light and vibrations of silica molecules and causes attenuation of short wavelength channels in wavelength multiplexed system[9]. Stimulated Brillouin Scattering is an interaction between light and sound waves in fibre and causes frequency conversion and reversal of propagation direction of light [9-11]. Cross-phase modulation (XPM) is an interaction via the nonlinear refractive index between the intensity of one light wave and the optical phase of other light waves [12]. Four wave mixing (FWM) is analogous to third order intermodulation distortion whereby two or more optical waves at different wavelength mix to produce new waves at other wavelength [9]. Stimulated Brillouin Scattering (SBS) and FWM processes are likely to impose severe restrictions on transmitter power in FDM system.

Coupling losses between the source/fibre, fibre/fibre and fibre/detector can cause attenuation in optical links. Losses can also occur from bending the fibre

too far, so that the light-ray hits the boundary at an angle less than the critical angle. As these loss mechanisms are extrinsic in nature, we can reduce them by taking various precautions. However, the fibre itself absorb some light and causes attenuation. The four main sources of attenuation : electron absorption , Rayleigh scattering , material absorption and impurity absorption.

Fibre chromatic dispersion , laser phase noise , relative intensity noise etc. the are other limitations [14-16]. The impulses of various wavelength travel at different speeds through the optical fibre and at the output the impulses get widening. Thus widening of the impulse depends on the spectral width of the source. This effect is known as chromatic dispersion . If the bit rate increases i.e. time slot decreases the impulses will overlap and no longer can be distinguished from eachother thus limiting transmission bit rate . The amount of dispersion is directly proportional to the fibre length. Chromatic dispersion results in limiting of the fibre transmission capability, due to variation in propagation time as a function of wavelength. This limitation due to laser phase noise may be overcome to some extent by using laser having narrow spectral width.

1.3 Review of Previous Work

There are increasing interests in optical fibre communication systems which operate at and above 10 Gb/s to meet the future demand for higher transmission capacity in different optical links. A sufficient amount of research works have been reported which encounters the degrading effects of laser phase noise, nonuniform FM response of DFB laser , nonlinear effect of optical fibre etc. on coherent and direct detection optical transmission system. A number of nonlinear effects are now being widely studied; for example, self phase

modulation (SPM), four wave mixing (FWM), cross phase modulation (XPM), stimulated Brillouin scattering (SBS), and stimulated Raman scattering (SRS).

Recent advances in optical signal transmission have already reached several thousand kilometers in the Gb/s range due to the use of in-line optical amplifier in different stages of the lightwave communication system [25]. The theoretical and experimental results have been reported at 10Gb/s with coherent and direct detection receivers with in line amplifiers [3,21-24]. The transmission distance in optical fibre communication has been greatly increased by the development of Erbium doped fibre amplifier[26]. The limitations of cascaded in-line amplifier systems are recently reported experimentally taking in to considerations the effects of linear ASE accumulation [27].

The main factor limiting the transmission distance in optical communication is now chromatic dispersion, specially at high bit rate i.e.10Gb/s transmission, pulse broadening causes ISI and thus reduce transmission distance. A signal transmitted very near the zero-dispersion wavelength undergoes remarkable noise enhancement due to four-wave mixing (FWM) between the signal and the amplified spontaneous emission (ASE) [28]. On the other hand, when the signal wave-length is away from the zero dispersion wave-length, the combined effect of self-phase modulation (SPM) and group velocity dispersion (GVD) causes wave-form distortion and limits the allowable transmission distance [29].

Fibre loss and chromatic dispersion in single mode optical fibres are two fundamental limitations in intensity modulated direct detection (IM/DD) optical fibre communication system design. In a 1310-nm wavelength window , standard single mode fibres have minimum chromatic dispersion but higher loss. A 1550-nm wavelength window is suitable for high bit rate, long-haul transmission owing to high capacities and low transmission loss of the fibre. Unfortunately, in this wavelength region the standard single mode fibre have a

typical chromatic dispersion of 15-20 ps/nm-km [17]. Several dispersion compensation techniques have been proposed based on Fabry -Perot etalons, two modes fibre and segmented core fibres [30-34]. These devices combined with the use of EDFAs have demonstrated successful compensation of chromatic dispersion.

An optical soliton compensate for the pulse distortion due to the nonlinear optical Kerr effect. In a linear regime, waveform distortion due to GVD can be removed by placing a GVD compensator in the receiver. Even in nonlinear regime, though it can not reproduce the initial wave-form because of the existence of SPM, GVD compensation is effective in reducing wave-form distortion and thus lengthening the transmission distance. The limitations on the performance of direct detection CPFSK system due to GVD is reported where the penalty is estimated from eye pattern at the output of the receiver [35].

1.4 Objectives of The Present Study

The main objective of this research is to analyze a point to point optical data transmission link with cascaded Erbium doped fibre amplifiers (EDFAs) with several dispersion compensation schemes to reduce the effect of GVD. The dispersion compensation is carried out by using compensating fibre in two cases: viz. lump compensation and even compensation . The objectives are

- to determine analytically the statistics of the resultant phase fluctuations due to chromatic dispersion and laser phase noise at the receiver output for NRZ and line-coded data patterns;
- to determine the expression for the bit error rate of CPFSK direct detection receiver using MZI as an OFD considering the effects of chromatic dispersion, accumulated ASE, laser phase noise when

diferent compensation schemes are used ;

- to evaluate the Bit Error Rate (BER) performance of the point to point optical link with NRZ data at a bit rate of 10 Gb/s with dispersion compensating fibre in lump as well as even compensation for different system parameters;
- to evaluate the BER performance of the system while using different linecoding schemes viz. MC, AMI, DM with and without dispersion;
- to evaluate the power penalty suffered by the system due to above system imperfections at $BER=10^{-9}$ and to determine optimum system parameters for a specified system penalty with NRZ data as well as with diferent linecoded data pattern;

1.5 Brief Introduction to This Thesis

A brief introduction to communication system is presented in Chapter-1 with an emphasis on optical communication system and a review of the research works currently going on in this field.

Chapter-2 presents performance analysis of a point to point optical link with cascaded EDFAs with several dispersion compensation schemes viz. Lump and even compensation with optical CPFSK modulation and Mach-Zehnder Interferometer (MZI) based direct detection receiver in the presence of group-velocity dispersion (GVD) and laser phase noise. The analysis is carried out for NRZ data as well as AMI, MC and DM encoded data pattern.

The results and discussions are presented in Chapter-3.

Conclusion and future scope of works are presented in Chapter-4.

CHAPTER-2

PERFORMANCE ANALYSIS OF A POINT TO POINT OPTICAL CPFSK TRANSMISSION SYSTEM

2.1 Overview

There is an increasing interest in optical fibre transmission systems which operate at and above 10 Gb/s to meet the future demand for higher transmission capacity in the exchange networks. But fibre chromatic dispersion is the key problem for lightwave transmission at 10 Gb/s of conventional single mode fibres which are optimized for transmission at 1310 nm. When distributed feedback lasers are frequency modulated for direct detection systems, producing significant wavelength chirp as well as intensity modulation, the resulting broad optical spectral width causes severe system degradation when fibre dispersion is present. Nearly all of the presently deployed fibres are optimized for 1310 nm operation and have a high dispersion of about 15 ps/nm.km in the low loss window near 1550 nm. Several theoretical and experimental works have been carried out on the effect of GVD on optical CPFSK and DPSK transmission systems [17-20].

In this chapter, performance analysis of a point to point optical data link is presented considering lump and even compensation. The analysis is carried out to evaluate the impact of fibre chromatic dispersion in optical transmission with cascaded optical amplifier system with CPFSK modulation and direct detection reception using a Mach-Zehnder Interferometer (MZI) as an optical frequency

discriminator (OFD). The analysis includes the effect of accumulated amplifiers spontaneous emission (ASE) noise, signal -ASE noise, ASE-ASE beat noise, laser phase noise and receiver noise. The statistics of the phase fluctuations due to chromatic dispersion in the presence of filtering effect and laser phase noise are determined analytically and the expression for the bit error probability of the direct detection FSK receiver is developed. The analysis is first carried out for NRZ data pattern and then extended to line-coded data patterns with three different line-coding schemes, viz. Alternate mark inversion (AMI), Miller code or Delay modulation (DM) and Manchester code(MC) to investigate the efficiency of the line-coding schemes in presence of dispersion. Following the theoretical analysis the bit error rate (BER) performance of the optical link is evaluated for NRZ and line-coded data pattern at a bit rate of 10 Gb/s for different system parameters. The power penalty suffered by the system due to above system imperfections at $BER=10^{-9}$ is evaluated. The optimum system parameters for a specified system penalty is also determined.

2.2 System Model

The system block diagram of optical transmission system with cascaded optical amplifier is shown in Fig. 2.1 and Fig. 2.2 for two different compensation schemes viz. lump compensation and even compensation respectively. In the first configuration, a GVD compensator is placed ahead of the direct detection receiver which is known as lump compensation. In the second configuration, GVD compensator is placed ahead of every amplifier and the receiver which is known as even compensation.

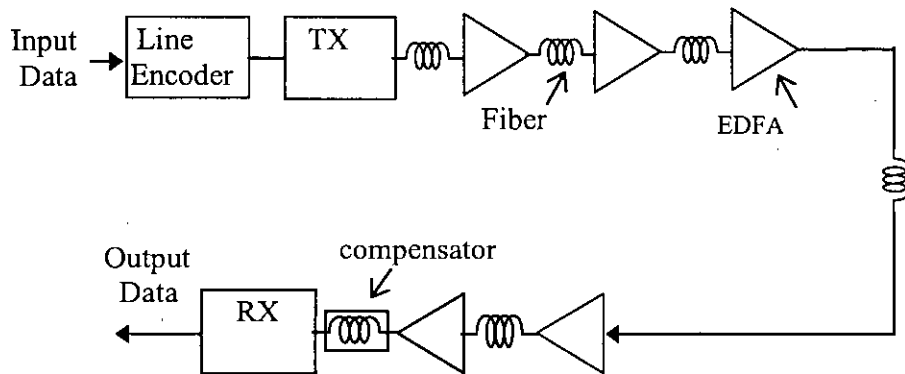


Fig. 2.1: Block diagram of optical transmission system with lump compensation.

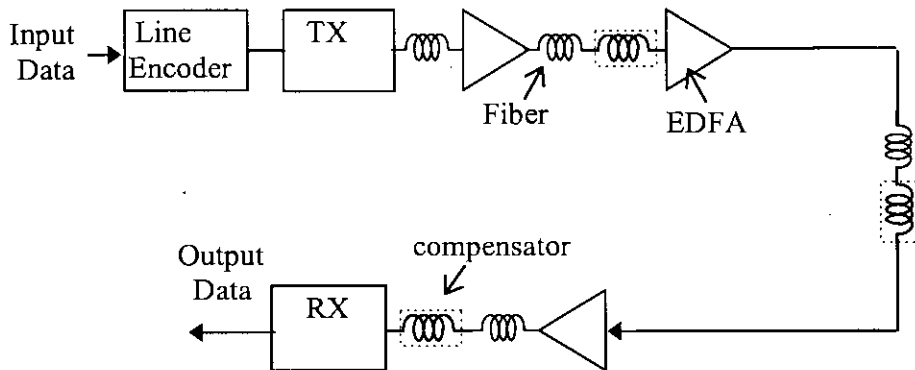


Fig. 2.2: Block diagram of optical transmission system with even compensation.

2.3 The Receiver Model

The block diagram of the FSK direct detection receiver with MZI considered for analysis is shown in Fig. 2.3. The MZI has two input ports, two 3dB couplers and two wave guide arms with length difference ΔL . A thin film heater is placed in one of the arms to act as a phase shifter, because light path length of heated wave guide arm changes due to the change of refractive index. The phase shifter is used for precise frequency tuning. Frequency spacing of the peak to bottom transmittance of the OFD is set equal to peak to peak frequency deviation $2\Delta f$ of the FSK signal. Consequently, the 'Mark' and the 'Space' appear at the two output ports of the OFD. These outputs are differentially detected by the balanced photodetectors. Thus the MZI acts as an optical filter and differentially detects the 'Mark' and 'Space' of received FSK signal which are then directly fed to a pair of photodetectors. The difference of the two photocurrents are applied to the pre-amplifier which is followed by an equalizer. The equalizer is required to equalize the pulse shape distortion caused by the photodetector capacitance and due to the input resistance and capacitance of the amplifier. After passing through the Gaussian low pass filter, the signal is detected at the decision circuit by comparing it with a threshold set to zero value.

2.3.1. MZI Characteristics

If $E(t)$ represents the signal input to the MZI, then the signals received at the output ports can be expressed as [36,37].

$$|E_2(t)| = |E(t)| \sin \left[\frac{k(l_2 - l_1)}{2} \right] \quad 2.1$$

and

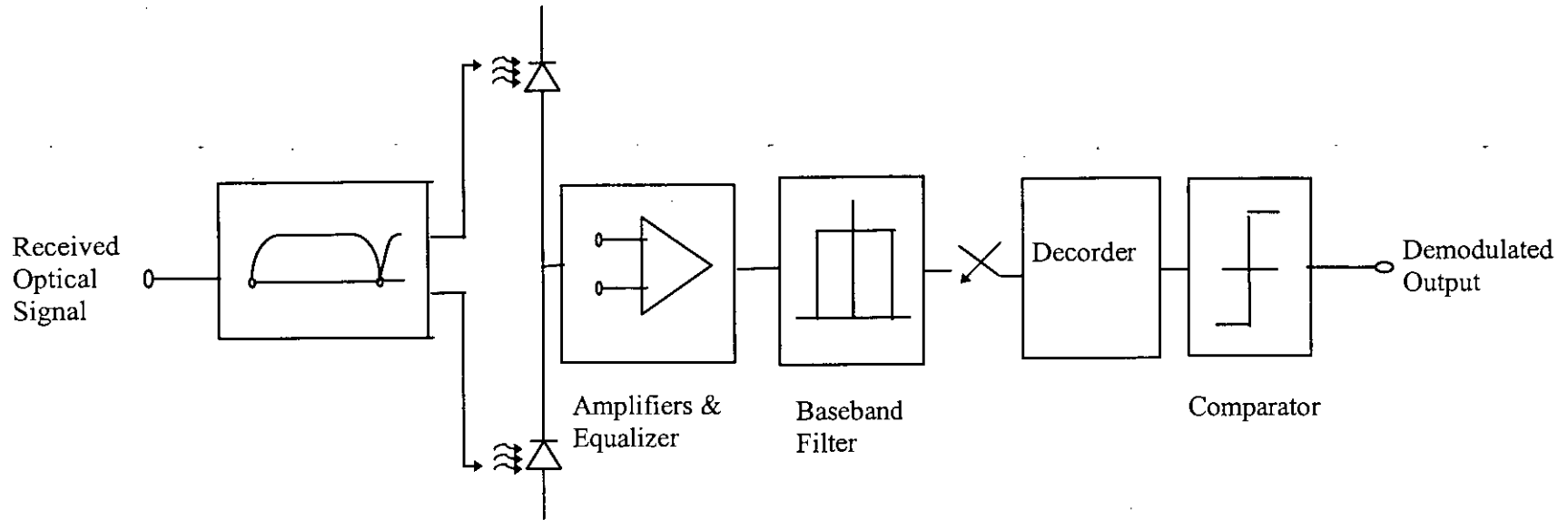


Fig. 2.3 Block diagram of an FSK direct detection receiver with a Mach-Zender interferometer (MZI) as an optical frequency discriminator (OFD)

$$|E_1(t)| = |E(t)| \text{Cos} \left[\frac{k(l_2 - l_1)}{2} \right] \quad 2.2$$

where l_1 and l_2 are the length of two arms of MZI and k is the wave number which can expressed as

$$k = \frac{w}{v} = \frac{2\pi}{\lambda} = \frac{2\pi f \eta_{eff}}{c}$$

η_{eff} , f and c are the effective refractive index of the wave guide, frequency of optical input signal and velocity of light in vacuum, respectively.

The transmittance of arm II of MZI is

$$T_{II}(f) = \frac{|E_2(t)|^2}{|E(t)|^2} = \text{Sin}^2 \left[\frac{k(l_2 - l_1)}{2} \right] = \text{Sin}^2 \theta \quad 2.3$$

and that of arm I of MZI is

$$T_I(f) = \frac{|E_1(t)|^2}{|E(t)|^2} = \text{Cos}^2 \left[\frac{k(l_2 - l_1)}{2} \right] = \text{Cos}^2 \theta \quad 2.4$$

where θ is the phase factor related to the arm path difference $\Delta L = l_2 - l_1$ and can be expressed as

$$\theta = \frac{k\Delta L}{2} = \frac{\pi f \eta_{eff} \Delta L}{c} \quad 2.5$$

Normally ΔL is chosen as

$$\Delta L = \frac{c}{4\eta_{eff} \Delta f} \quad 2.6$$

Therefore, $\theta = \frac{\pi f}{4\Delta f}$

Then we get

$$T_{II}(f) = \text{Sin}^2 \left(\frac{\pi f}{4\Delta f} \right) \quad 2.7$$

and

$$T_I(f) = \text{Cos}^2 \left(\frac{\pi f}{4\Delta f} \right) \quad 2.8$$

The outputs of the MZI are therefore anti-symmetric and are shown in Fig 2.4.

For an MZI, used as an OFD, Δf is so chosen that [36,37] $\Delta f = \frac{f_c}{2n+1}$, f_c is the carrier frequency of the FSK signal and n is an integer. The 'mark' and 'space' of FSK signals are represented by f_1 and f_2 respectively where $f_1 = f_c + \Delta f$ and $f_2 = f_c - \Delta f$

Therefore when 'mark' f_1 is transmitted

$$T_I = 1 \text{ and } T_{II} = 0$$

Similarly, for transmission of 'space'

$$T_I = 0 \text{ and } T_{II} = 1$$

Thus, two different signals f_1 and f_2 can be extracted from two output ports of MZI.

The MZI is used in our analysis as an OFD for a multichannel WDM/FDM system, can be fabricated utilizing the periodicity of the transmittance versus frequency characteristic of an MZI [36,37].

2.4 Theoretical Analysis for Optical Direct Detection CPFSK

2.4.1 FSK with NRZ data

The optical FSK signal input to the fibre is given by

$$E_{in}(t) = \sqrt{2P_T} \exp\left[j\{2\pi f_c t + \phi_s(t) + \phi_n(t)\}\right] \quad 2.9$$

where f_c is the optical frequency, P_T represents the transmitted optical signal power, $\phi_s(t)$ is the angle modulation, $\phi_n(t)$ is the phase noise of the transmitting laser. Here $\phi_s(t)$ is given by

$$\phi_s(t) = 2\pi\Delta f \int_{-\infty}^t I(t) dt \quad 2.10$$

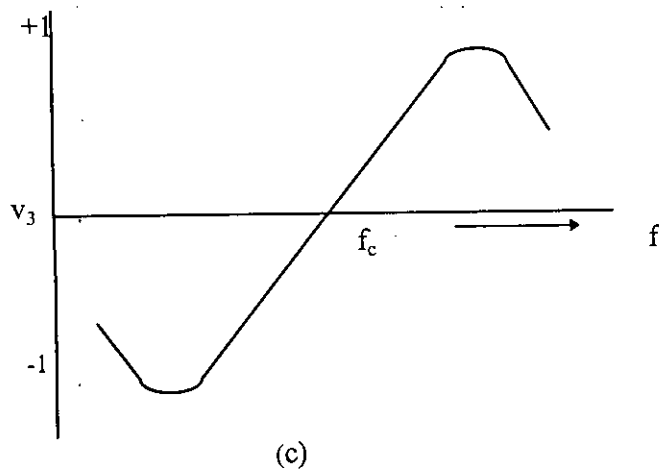
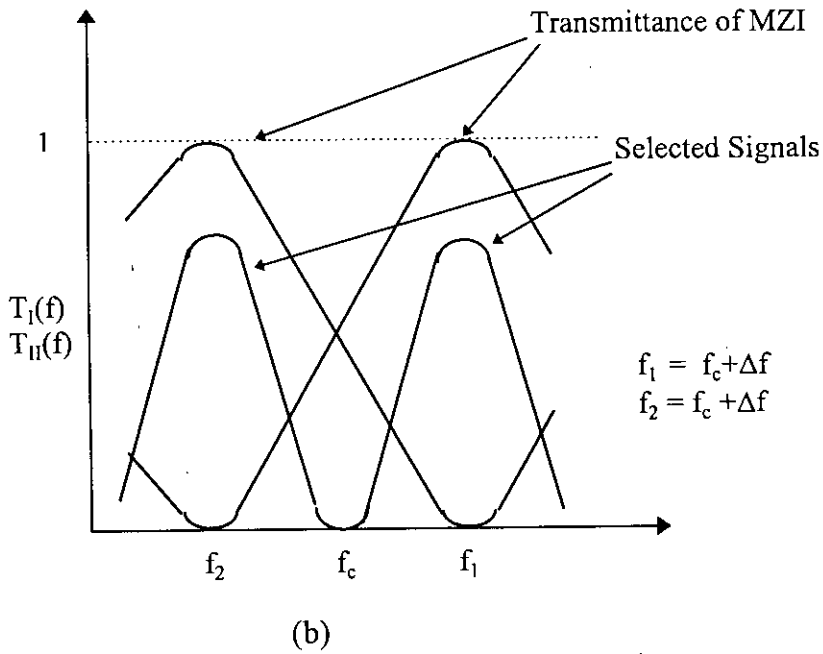
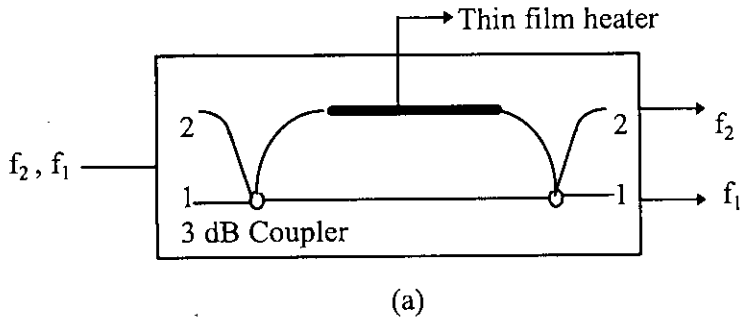


Fig.2.2 (a)An MZI with large ΔL or narrow wavelength spacing,(b)Transmittance characteristics of an MZI and (c) Differential output of the balanced receiver.

where $I(t) = \sum_k a_k p(t - kT)$; $p(t)$ represents the elementary pulse shape, $a_k = \pm 1$ is the random NRZ bit pattern and Δf is the peak frequency deviation. For NRZ data $p(t)$ is a rectangular pulse of unit amplitude.

The single mode fibre transfer function due to chromatic dispersion [17] is given by :

$$H_f(f) = \exp(-j\alpha f^2) \quad 2.11$$

where $\alpha = \frac{\pi D_c L \lambda^2}{c}$, D_c is the fibre chromatic dispersion, λ is the optical wavelength, c is the speed of light and L is the length of fibre. The fibre impulse response $h_f(t)$ is given by $h_f(t) = F^{-1}[H(f)]$ where F denotes Fourier transformation.

2.4.1.1 Lump Compensation

In this scheme, the compensation for chromatic dispersion is carried out by placing a dispersion compensating fibre at the end of the transmission fibre. The transmission fibre is a non-dispersion-shifted (NDS) fibre with dispersion coefficient D_c of 15ps/nm-km and have a transfer function given by

$$H_f(f) = \exp\left[\frac{-j\pi D_c L \lambda^2 f^2}{c}\right] \quad 2.12$$

where, L is the total length of fibre. The transfer function of the compensating fibre is given by

$$H_c(f) = \exp\left[\frac{-j\pi D'_c L' \lambda^2 f^2}{c}\right] \quad 2.13$$

where D'_c is the dispersion coefficient and L' is the length of the compensating fibre.

The overall transfer function is then given by $H_o(f) = H_f(f).H_c(f)$

2.4.1.2 Even Compensation

In case of even compensation, the effect of dispersion is compensated in each section by putting a compensating fibre at the end of each section before the optical amplifier. The transfer function of the transmission fibre is given by

$$H'_f(f) = \exp\left[\frac{-j\pi.D_c.L_a.\lambda^2.f^2}{c}\right] \quad 2.14$$

where L_a is the length of each fibre section and $L_a = L/N$ where L is the total fibre length and N is the number of sections. The transfer function of the compensating fibre can be obtained as

$$H'_c(f) = \exp\left[\frac{-j\pi.D'_c.L'_a.\lambda^2.f^2}{c}\right] \quad 2.15$$

where L'_a is the length of the compensating fibre in each section.

The overall transfer function of the fibre link is given by

$$H_o(f) = \prod_{i=1}^N H'_f(f).H'_c(f) \quad 2.16$$

The signal at the end of the fibre section i.e. at the input to the Mach-Zehnder interferometer is given by

$$\begin{aligned} E_o(t) &= E_{in}(t) \otimes h_o(t) \\ &= \sqrt{2P_s GL} \exp\left[j\{2\pi f_c t + \phi(t)\}\right] \otimes h_o(t) \end{aligned} \quad 2.17$$

Where $h_o(t) = F^{-1}\{H_o(f)\}$, F^{-1} denotes inverse Fourier transformation, P_s is the received optical power and $\phi(t) = \phi_s(t) + \phi_n(t)$

The signal phase $\phi_o(t)$ at the input to MZI is given by [38]

$$\begin{aligned} \phi_o(t) &= Re \left[\int_{-\infty}^t h_o(\tau).exp\{j\phi(t-\tau)\}d\tau \right] + \sum_{n=2}^{\infty} \frac{1}{n!} Im(j^n f_n) \\ &= \theta_l(t) + \theta_{nl}(t) \end{aligned} \quad 2.18$$

where Re and Im denotes the real and imaginary parts respectively, $\theta_l(t)$

represents the linear filtering term and $\theta_{nl}(t)$ represents the non-linear filtering terms consisting of the cross-term and the intermodulation terms. The expression for f_n are given in reference[38]. Assuming linear phase approximation [20] the linearly filtered phase $\theta_l(t)$ can be rewritten as

$$\begin{aligned}\theta_l(t) &= Re \left[\int_{-\infty}^t h_o(\tau) \phi(t-\tau) d\tau \right] \\ &= Re \left[\int_{-\infty}^t h_o(\tau) \phi_s(t-\tau) d\tau \right] + Re \left[\int_{-\infty}^t h_o(\tau) \phi_n(t-\tau) d\tau \right] \\ &= \theta_s(t) + \theta_n(t)\end{aligned}\tag{2.19}$$

where $\theta_s(t)$ and $\theta_n(t)$ are the filtered output signal phase and phase noise respectively.

2.4.1.3 The Receiver Output Signal

The photodetector output current is then obtained as

$$\begin{aligned}i(t) &= R_d \left| E_s(t) + E_{sp}(t) \right|^2 \\ &= i_s(t) + i_{s-sp}(t) + i_{sp-sp}(t) + i_{th}(t) + i_{sh}(t)\end{aligned}\tag{2.20}$$

where $i_s(t)$ represents the signal current, $i_{s-sp}(t)$ is the current due to signal-spontaneous emission beat noise, $i_{sp-sp}(t)$ is the spontaneous-spontaneous beat noise, $i_{th}(t)$ is the receiver thermal noise and $i_{sh}(t)$ is the photodetector shot noise.

The power spectral density of the different beat-noise components are given by :

$$S_{s-sp} = 4R_d P_s q G (G-1) L_f^2 N_{sp} N [\delta(f) \otimes G_{FSK-PN}(f)]\tag{2.21}$$

$$S_{sp-sp} = 2q^2 N^2 N_{sp}^2 (G-1)^2 L_f^2\tag{2.22}$$

where $\delta(f)$ is a delta function in frequency, G is the gain of the EDFA in each

section, L_f is the fibre loss, q is the electronic charge, N is the number of amplifiers, N_{sp} spontaneous emission factor, $G_{FSK-PN}(f)$ represents the normalized power spectral density (PSD) of the phase noise corrupted FSK signal.

For a ‘mark’ transmission, the current at output of balanced photodetector is[39]

$$i_m(t) = R_d P_s \text{Cos}[2\pi f_c \tau + \Delta\theta_s(t) + \Delta\theta_n(t)] \quad 2.23$$

where $\Delta\theta_s(t) = \theta_s(t) - \theta_s(t - \tau)$, τ is the time delay between the two branches of the MZI and $\Delta\theta_n(t) = \theta_n(t) - \theta_n(t - \tau)$.

From (2.19) $\theta_s(t)$ can be expressed as

$$\begin{aligned} \theta_s(t) &= \phi_s(t) \otimes h_o(t) \quad 2.24 \\ &= 2\pi\Delta f \int_{-\infty}^t I(t) \otimes h_o(t) dt \\ &= 2\pi\Delta f \int_{-\infty}^t \sum_k a_k p(t - kT) \otimes h_o(t) dt \\ &= 2\pi\Delta f \int_{-\infty}^t \sum_k a_k g(t - kT) dt. \end{aligned}$$

where $g(t) = p(t) \otimes h_o(t)$

Thus the chromatic dispersion produces distortion of the optical pulse shape.

Therefore,

$$\begin{aligned} \Delta\theta_s(t) &= \theta_s(t) - \theta_s(t - \tau) \quad 2.25 \\ &= 2\pi\Delta f \int_{t-\tau}^t \sum_k a_k g(t - kT) dt \end{aligned}$$

Thus the output of the balanced photodetectors is

$$i(t) = R_d P_s \text{Cos} \left[2\pi f_c \tau + 2\pi\Delta f \int_{t-\tau}^t \sum_k a_k g(t - kT) dt + \Delta\theta_n(t) \right] \quad 2.26$$

Therefore $i(t)$ is given by

$$i(t) = R_d P_s \text{Cos} \left[2\pi f_c \tau + 2\pi \Delta f \int_{t-\tau}^t a_o g(t) dt \right] \quad 2.27$$

$$+ 2\pi \Delta f \int_{t-\tau, k \neq 0}^t \sum a_k g(t - kT) dt + \Delta \theta_n(t)$$

For 'mark' transmission ($a_o = +1$) at any sampling instant can be expressed as

$$i(t) = R_d P_s \text{Cos} \left[2\pi f_c \tau + \frac{\pi}{2} - \frac{\pi}{2} + 2\pi \Delta f \tau q(t) + 2\pi \Delta f \int_{t-\tau, k \neq 0}^t \sum a_k g(t - kT) dt + \Delta \theta_n(t) \right]$$

$$= R_d P_s \text{Cos} \left[2\pi f_c \tau + \frac{\pi}{2} - \frac{\pi}{2} + \frac{\pi}{2} q(t) + \frac{\pi}{2} \sum_{k \neq 0} a_k g(t - kT) dt + \Delta \theta_n(t) \right] \quad 2.28$$

where for optimum demodulation, $\tau = \frac{T}{2h}$ and $h (= 2\Delta f T)$ is the modulation index

and $q(t)$ is defined as

$$q(t) = \frac{1}{\tau} \int_{t-\tau}^t g(t_1) dt_1 \quad 2.29$$

$$\Delta \theta_n(t) = 2\pi \int_{t-\tau}^t \mu(t_1) dt_1 \quad 2.30$$

$\mu(t)$ is a zero mean Gaussian frequency noise process having two sided flat PSD of height $\frac{\Delta \nu}{2\pi}$, $\Delta \nu$ being the transmitting laser linewidth.

Denoting the phase noise due to chromatic dispersion by $\Delta \theta_{CD}$ as

$$\Delta \theta_{CD}(t) = -\frac{\pi}{2} + \frac{\pi}{2} q(t) + \frac{\pi}{2} \sum_{k \neq 0} a_k q(t - kT) dt \quad 2.31$$

$$= \bar{\theta}_{CD} + \frac{\pi}{2} \sum_{k \neq 0} a_k q(t - kT) dt$$

where $\bar{\theta}_{CD} = -\frac{\pi}{2} + \frac{\pi}{2} q(t)$; the output current $i_m(t)$ can be expressed as

$$i_m(t) = R_d P_s \text{Cos} \left[2\pi f_c \tau + \frac{\pi}{2} + \Delta \theta_{CD} + \Delta \theta_n(t) \right] \quad 2.32$$

$\Delta \theta_{CD}(t)$ is induced by the GVD and $\Delta \theta_n(t)$ accounts for the phase distortion due to laser phase noise.

2.4.1.4 Bit Error Rate Expression

Under ideal CPFSK demodulation condition $w_c \tau = (2n + 1) \frac{\pi}{2}$ where n is an integer and $2\pi \Delta f \tau = \frac{\pi}{2}$ for NRZ data.

The output signal corresponding to the 'mark' and 'space' transmission are

$$i_m(t) = R_d P_s [x(t)] \quad \text{and} \quad i_s(t) = -R_d P_s [x(t)] \quad 2.33$$

where $x(t) = \text{Cos}[\Delta\phi(t)]$ describe the phase noise induced interferometric intensity noise and $\Delta\phi(t) = \Delta\theta_{cd}(t) + \Delta\theta_n(t)$

The output of the low-pass filter for 'mark' transmitted at a sampling time t is

$$i(t) = R_d P_s \text{Cos}[\Delta\phi(t)] + n(t) \quad 2.34$$

where $n(t)$ is total noise power consists of the filtered output noise contributed by the photodetector quantum shot noise, the interferometric noise due to input intensity fluctuation, receiver thermal noise and other beat noise components.

The total noise power spectral density is given by

$$S_n(f) = S_{pd}(f) + S_{pdi}(f) + S_{th}(f) + S_{s-sp}(f) + S_{sp-sp}(f) \quad 2.35$$

where

$$S_{pd}(f) = q R_d P_s \quad 2.36$$

$$S_{pdi}(f) = 0.5 R_d P_s \left[S_x(f) - \bar{x}^2 \delta(f) \right] \quad 2.37$$

$$S_{th}(f) = i_{th}^2 \quad 2.38$$

and \bar{x} represent the PSD and the mean value of $x(t)$ respectively.

The total noise power is then obtained as

$$\sigma_m^2 = \sigma_s^2 = \int_{-\frac{B_c}{2}}^{\frac{B_c}{2}} S_n(f) |H_{LP}(f)|^2 df \quad 2.39$$

where $H_{LP}(f)$ represents the transfer function of the receiver low-pass filter which

is assumed to be Gaussian having bandwidth $B_e = 0.75B_r$.

$$\text{Let } Q = \frac{i_m - i_s}{\sigma_m + \sigma_s} \quad 2.40$$

Then the conditional bit error rate can be expressed as

$$P(e|\Delta\phi) = 0.5 \operatorname{erfc}\left(\frac{Q}{\sqrt{2}}\right) \quad 2.41$$

The average bit error rate of a direct detection CPFSK system is

$$BER = 0.5 \int_{-\infty}^{\infty} \operatorname{erfc}\left(\frac{Q}{\sqrt{2}}\right) P_{\Delta\phi}(\Delta\phi) d(\Delta\phi) \quad 2.42$$

where $P_{\Delta\phi}(\Delta\phi)$ is the probability density function of $\Delta\phi$

Using Gauss-quadrature rule, the BER can be computed as

$$BER = 0.5 \sum_{i=1}^N \int_{-\infty}^{\infty} w_i \operatorname{erfc}\left[\frac{2\left\{R_d P_s \cos(\Delta\theta_{cd}^i + \Delta\theta_n)\right\}}{\sqrt{2}\sigma}\right] P_{\Delta\theta_n}(\Delta\theta_n) d(\Delta\theta_n) \quad 2.43$$

where the weights w_i and the nodes $\Delta\theta_{cd}^i$ are evaluated from the knowledge of moments of the random process $\Delta\theta_{cd}(t)$ and $P_{\Delta\theta_n}(\Delta\theta_n)$ is the Gaussian pdf of the laser phase noise at the output with zero mean and variance $\sigma_{ph}^2 = 2\pi\Delta\nu\tau$.

2.4.2 Self Phase Modulation (SPM)

In the presence of SPM induced by GVD, the overall phase impulse response of fibre can be obtained by using the Split-Step-Fourier method as follows.

Utilizing PM-AM conversion induced by GVD [41] and the resulting generated SPM, the Fourier transform of the output phase $\phi_{out}(\omega)$ and the output power fluctuation $\xi_{out}(\omega)$, under linear phase approximation [38], are related to the corresponding transforms of the input quantities viz. $\phi_{in}(\omega)$ and $\xi_{in}(\omega)$, through a

transfer function matrix :

$$\begin{bmatrix} \phi_{out}(\omega) \\ \xi_{out}(\omega) \end{bmatrix} = B_{SPM}(N, \omega) \begin{bmatrix} \phi_{in}(\omega) \\ \xi_{in}(\omega) \end{bmatrix} \quad 2.44$$

where, $B_{SPM}(N, \omega)$ is the transfer function of a system of N cascaded segments each of length L_k . Corresponding to an input phase excitation $\phi_{in}(t)$, the output phase response $\phi_{out}(t)$ can be directly obtained from Eqn.2.44. By virtue of the validity of linear phase approximation in a practical situation, we introduce an equivalent phase impulse response $h'_f(t) = F^{-1}[B'^1_{SPM}(N, \omega)]$ where the 2×2 matrix $B_{SPM}(N, \omega) = G_N A_N(\omega) \dots G_1 A_1(\omega)$, G_i is a gain matrix of the i-th amplifier and F^{-1} denotes the inverse Fourier transform.

The matrix A_k can be formed as : $A_k = \lim_{q \rightarrow \infty} A^q \dots A^1$, and the matrix A^p is given by

$$A^p = \begin{bmatrix} \cos(\omega^2 F_k) & -2P_0 e^{-p\alpha\Delta L} \sin(\omega^2 F_k) \\ \frac{e^{p\alpha\Delta L} \sin(\omega^2 F_k)}{P_0} + \gamma\Delta L_k & \cos(\omega^2 F_k) \end{bmatrix} \quad 2.45$$

$$\text{where, } F_k = \beta \frac{k}{2} \Delta L_k / 2 \quad 2.46$$

and $\beta \frac{k}{2}$ is the dispersion coefficient in ps^2/km in the k-th segment, γ is the fibre nonlinear coefficient, P_0 is the signal power input to the fibre, α is the fibre attenuation, and $\Delta L_k = L_k / q$.

The effect of SPM in presence of GVD can be evaluated by using analytical approach presented in sec. 2.4.1 by replacing the fibre response $h_f(t)$ by $h'_f(t)$ which include the effect of SPM and GVD.

2.4.3 CPFSK System With Line Coding

It is known that appropriate line-coding of the laser driving signal can overcome the adverse effect of non-uniform FM response of the transmitting laser. Three different line-coding schemes are considered here, viz. , Alternate-Mark-Inversion (AMI), Delay Modulation or Miller code (DM), and Manchester or biphase code (MC) to investigate their efficacy in presence of fibre chromatic dispersion.

AMI Encoding

This is a ternary line code. The modulator has $q=2$ states, say, Σ_+ and Σ_- , and the source is binary. The modulator response to a source symbol '0' with a zero waveform and to a source symbol '1' with waveform $s(t)$ or $-s(t)$, according to whether its state is Σ_+ or Σ_- respectively. Source symbols '1' make the modulator change its state. The tabular and state diagram representation of this signal are provided in Fig. 2.5(a).

It is intuitive that this encoding method has the advantage of reducing the dc component of the signal because of a pulse of one polarity is always followed by a pulse of opposite polarity. Moreover, a single transmission error will always give rise to a bipolar violation, that is, the presence of a pulse that does not satisfy the bipolar encoding rule. This property does not represent a powerful error detection scheme. Nevertheless, it allows the monitoring of quality of the transmission link without the need for any information on the transmitted data. Finally, transmission of long sequences of zeroes results in long period without timing information. The polar code does not present good self locking capabilities, and one must resort to scrambling the transmitted sequence.

$\sigma_n \backslash \lambda_n$	Σ_+	Σ_-
0	0	0
1	$s(t)$	$-s(t)$

$\sigma_n \backslash \lambda_n$	Σ_+	Σ_-
0	Σ_+	Σ_-
1	Σ_-	Σ_+

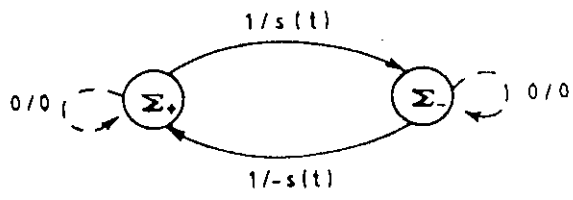


Fig. 2.5 (a) Tabular and state diagram of Alternate Mark inversion (AMI) line code.

$\sigma_n \backslash \lambda_n$	Σ_1	Σ_2	Σ_3	Σ_4
0	$s_4(t)$	$s_4(t)$	$s_1(t)$	$s_1(t)$
1	$s_2(t)$	$s_3(t)$	$s_2(t)$	$s_3(t)$

$\sigma_n \backslash \lambda_n$	Σ_1	Σ_2	Σ_3	Σ_4
0	Σ_4	Σ_4	Σ_1	Σ_1
1	Σ_2	Σ_3	Σ_2	Σ_3

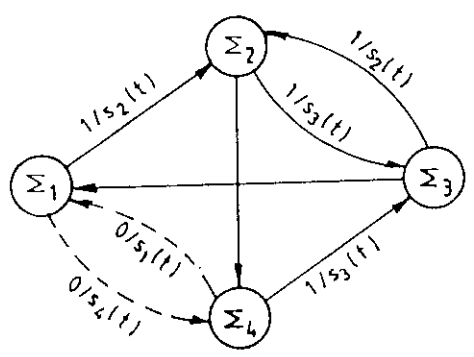
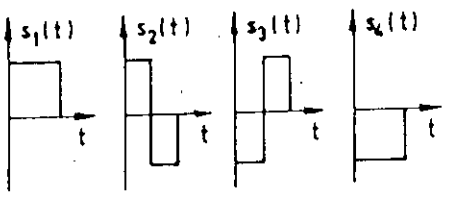


Fig. 2.5 (b) Tabular and state diagram of Delay Modulation (DM) line code.

DM Encoding

This code is also known as Miller code. The modulator has four encoder states and the source is binary. Four baseband signals are available. Which one is transmitted depends on both the present digit and the previous transmitted bit. The encoding rule can be followed in accordance with the tabular and state diagram of the encoder shown in Fig. 2.5(b). Each state is identified by the label of the previously transmitted signal. Each transmission between two states is represented with a solid arrow if a 'one' is to be encoded and with a dashed arrow if a 'zero'. The label on each arrow indicates the generated signal. The possible waveforms are also shown in Fig. 2.5(b).

Manchester Encoding

It uses two antipodal signals. The encoding is followed as shown on the tabular and state diagram of the encoder shown in Fig. 2.5(c). Each state is identified by the label of the previously transmitted signal. The power spectral density of the NRZ, AMI, MC, and DM codes are shown in Fig. 2.6 for the case of equally likely binary bit. Notice that the latter three codes show a spectral minimum at $f=0$. This desirable property is an important feature and acts as a countermeasure to the effect of nonuniform FM response of laser. When comparing MC and DM, notice that the latter has its power concentrated in a bandwidth that is less than the one-half the symbol rate and thus presents a higher bandwidth efficiency.

Analytical Approach

Let $g(t)$ is the overall impulse response of the optical link without the use of linecoding and $g'(t)$ is the overall impulse response with line-coding. Then by definition we can write the linecoding effect in the frequency domain as

$$G'(f) = G''(fT) \cdot G(f) \quad 2.48$$

$\alpha_n \backslash \sigma_n$	Σ_1	Σ_2
0	$S(t)$	$S(t)$
1	$-S(t)$	$-S(t)$

$\alpha_n \backslash \sigma_n$	Σ_1	Σ_2
0	Σ_1	Σ_1
1	Σ_2	Σ_2

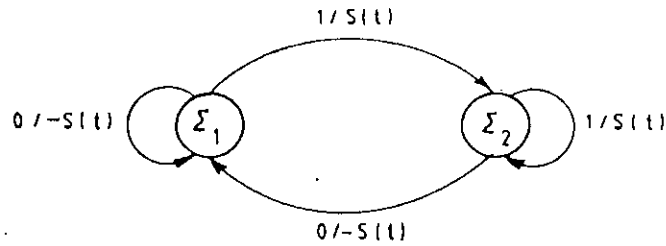


Fig. 2.5 (c) Tabular and state diagram of Manchester Code (MC).

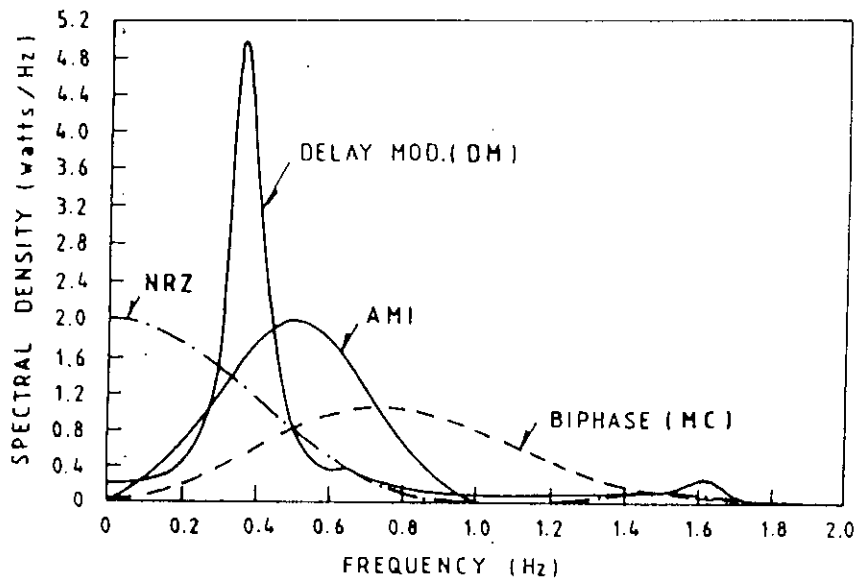


Fig. 2.6 Power spectral density of different line codes : NRZ, AMI, DM and MC.

Where

$$G''(fT) = \sum_{n=0}^{K-1} g'_n e^{-j2\pi n f T} \quad 2.49$$

is the transfer function of the discrete linear system. Thus the encoder is a filter with transfer function $G''(fT)$ which is the Fourier transform of the pulse shaping function $g''(t)$.

For the linecoded signal, the pulse shaping function $g''(t)$ can be obtained as [40]

$$g''(t) = F^{-1}\{G''(f)\} \quad 2.50$$

where $G''(f)$ is given by

For AMI :

$$G''(f) = 1 - e^{-j2\pi f T} \quad 2.51$$

For DM :

$$G''(f) = \frac{(3+2\cos\alpha + \cos 2\alpha - \cos 3\alpha) + j(6\sin 2\alpha + \sin\alpha + 3\sin 3\alpha + 4\sin 4\alpha)}{9+12\cos 2\alpha + 4\cos 4\alpha} \quad 2.52$$

For MC :

$$G''(f) = 1 - e^{-j\pi f T} \quad 2.53$$

Where $\alpha = \pi f T$. For DM and MC, $g(t)$ is a rectangular pulse of duration $T/2$.

The bit error rate performance of the linecoded FSK system can be evaluated following the similar approach provided in sec. 2.4.1 by replacing the equivalent pulse shape $P(t)$ by $P'(t)$ gives as

$$\begin{aligned} P'(t) &= F^{-1}[P'(f)] \\ &= F^{-1}[P(f) \cdot G''(f)] \end{aligned} \quad 2.54$$

CHAPTER-3

RESULTS AND DISCUSSION

Following the theoretical analysis presented in chapter-2 the performance results for point to point optical CPFSK transmission link are evaluated at a bit rate of 10 Gb/s for two different compensation schemes for dispersion compensation viz. lump compensation and even compensation. The results are evaluated for different fibre span , compensator span, number of fibre section, different modulation index and system parameters. The parameters of the single mode fibre used for numerical computations are: chromatic dispersion coefficient $D_c = 15 \text{ Ps/nm-km}$, dispersion coefficient of compensating fibre $D'_c = 15 \text{ Ps/nm-km}$, wavelength $\lambda = 1550 \text{ nm}$.

The bit error rate (BER) performance of point to point optical direct detection CPFSK link with lump compensation is depicted in Fig. 3.1 in presence of ASE noise of the cascaded EDFAs, and receiver noises considering the effect of fibre chromatic dispersion. The BER curve for $D_c=0$ is also plotted is the reference receiver sensitivity. The BER is plotted as a function of the received optical power P_s (dBm) and the receiver sensitivity is defined as the optical power required to achieve a BER of 10^{-9} . The BER values are computed for a fibre length $L=40\text{km}$ and different values of compensator length i.e. $L' = 0, 20, 30, 40$ and 60km for a modulation index $h = 1$. The figure reveals that the BER decreases with increase in received power. For a given value of BER, the required power is maximum without compensation ($L' = 0$) and as the compensator length L' increases the value of required received power

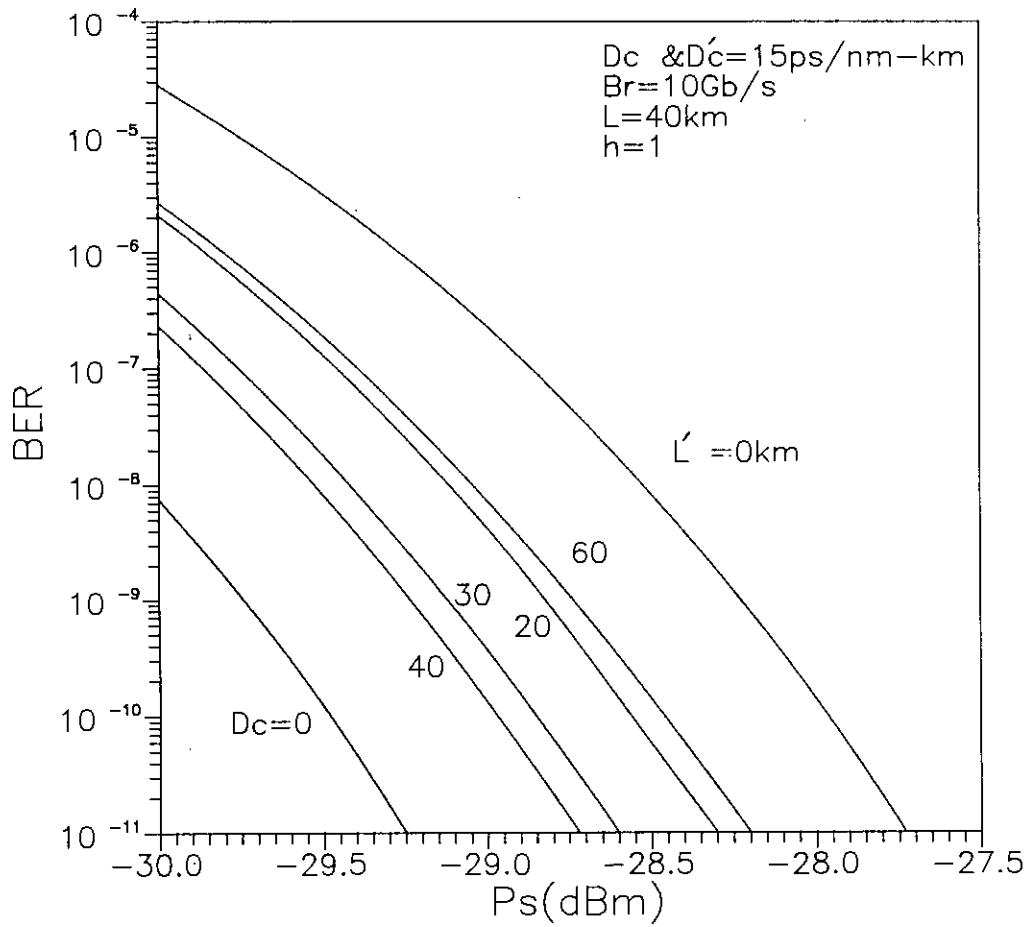


Fig. 3.1 The bit error rate (BER) performance of a point to point optical direct detection CPFSK link with lump compensation at a bit rate of 10 Gb/s with dispersion coefficient $D_c \text{ \& } D'_c = 15 \text{ ps/nm-km}$, fibre length $L = 40 \text{ km}$ at an wavelength of 1550 nm and modulation index $h = 1$ for several values of compensator length.

decreases. The required received power is minimum for a compensator length $L'=40\text{km}$ i.e. when the dispersion fibre length equals the compensator length. Further increase in compensator length causes an increase in received signal power. This is due to over compensation which causes further increase in penalty.

The bit error rate (BER) performance results of a point to point optical link with lump compensation are also shown in Fig. 3.2 and Fig. 3.3 in presence of ASE noise due to the cascaded EDFAs, and receiver noises in presence of fibre chromatic dispersion for fibre length $L=60\text{km}$ and 80km respectively and modulation index $h=1$. It is also observed in Fig. 3.2 and Fig. 3.3 that for a given value of BER the required signal power decreases with the increase of compensator length until it equals the fibre length and further increase in compensator length causes increased signal power. Thus it is found from Fig. 3.1 through Fig. 3.3 that for lump compensation received signal power decreases with increase of compensator length and penalty reduces to a minimum value when the length of the compensating fibre equals the dispersive fibre length.

The plots of penalty in signal power due to fibre chromatic dispersion without any compensation for different fibre length is also shown in Fig. 3.4. The plots of penalty in signal power due to fibre chromatic dispersion with lump compensation scheme at $\text{BER}=10^{-9}$ for modulation index $h = 1$ is depicted in Fig. 3.5. The penalty is plotted as a function of $D'_c L'$ (product of D'_c and L' of compensator) for fibre length $L=40, 60$ and 80km . Let us compare the penalty of Fig. 3.4 and Fig. 3.5. Without compensation the penalty increases continuously with the increases of fibre length. But with lump compensation penalty decreases with increase in compensator length upto a minimum value and then again increases. The plots of penalty in signal power due to fibre

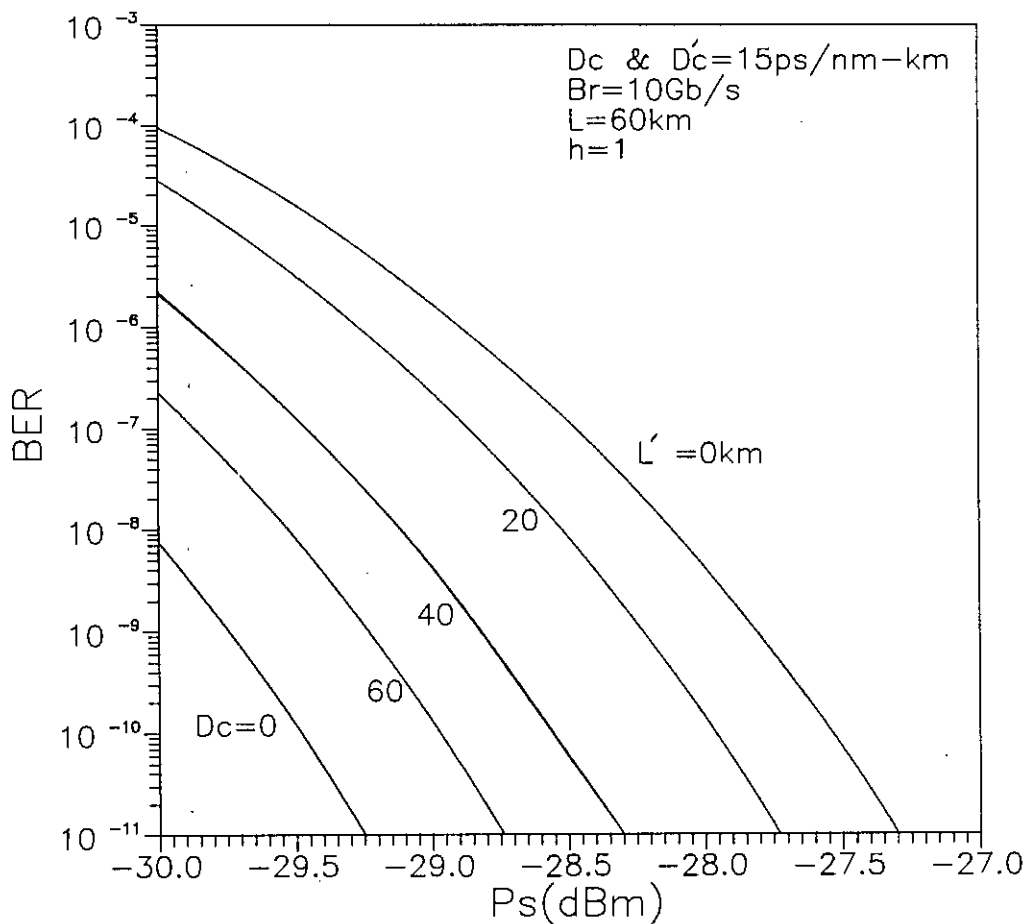


Fig. 3.2 The bit error rate (BER) performance of a point to point optical direct detection CPFSK link with lump compensation at a bit rate of 10 Gb/s with dispersion coefficient $D_c \text{ \& } D'_c = 15 \text{ ps/nm-km}$, fibre length $L = 60 \text{ km}$ at an wavelength of 1550 nm and modulation index $h = 1$ for several values of compensator length.

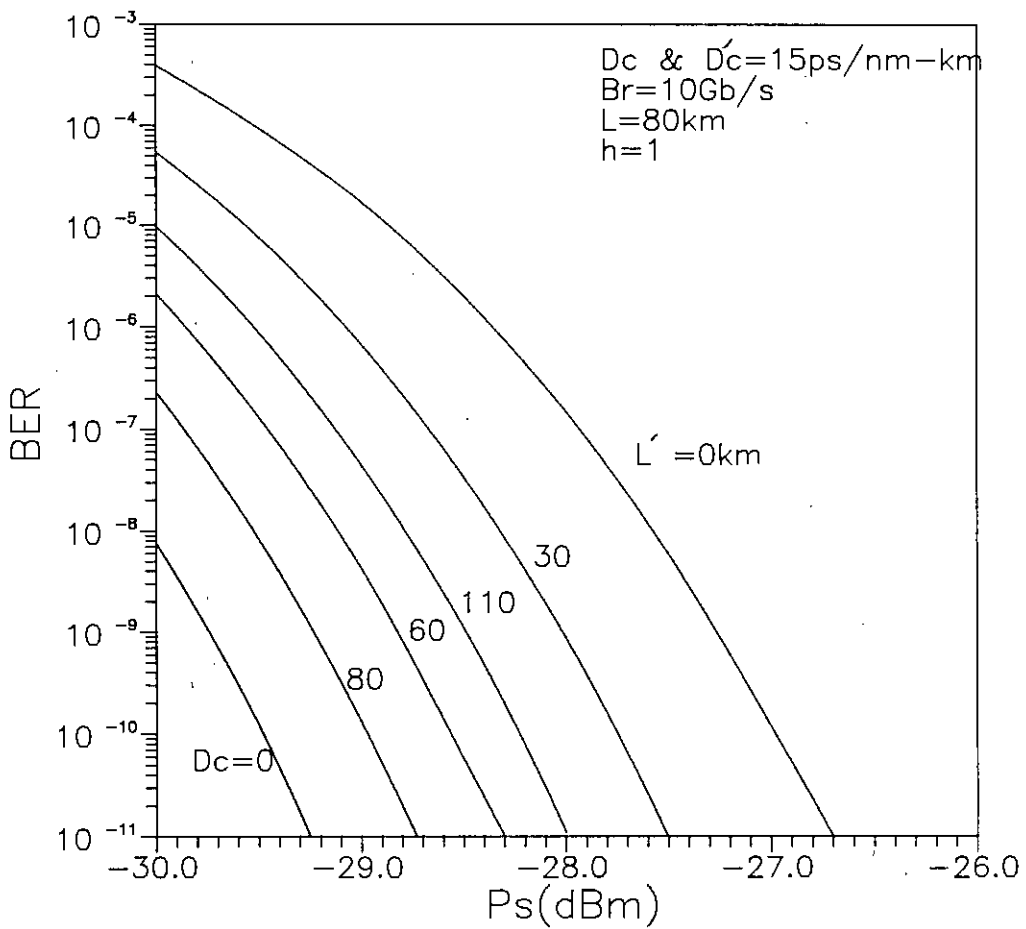


Fig. 3.3 The bit error rate (BER) performance of a point to point optical direct detection CPFSK link with lump compensation at a bit rate of 10 Gb/s with dispersion coefficient $D_c \text{ \& } D'_c = 15 \text{ ps/nm-km}$, fibre length $L = 80 \text{ km}$ at an wavelength of 1550 nm and modulation index $h = 1$ for several values of compensator length.

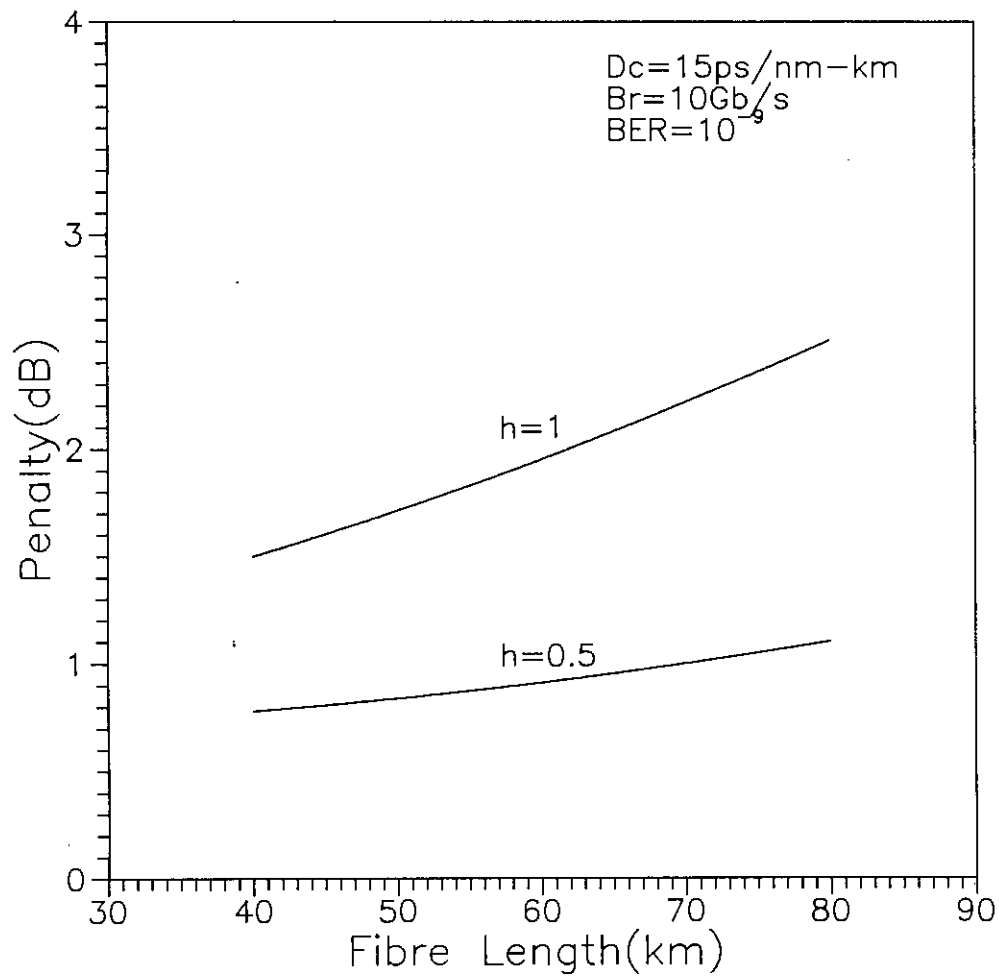


Fig. 3.4 Plots of penalty in signal power due to fibre chromatic dispersion for a point to point optical CPFSK link without any compensation versus with fibre length L at $\text{BER} = 10^{-9}$ and modulation index $h=0.5$ and $h=1$.

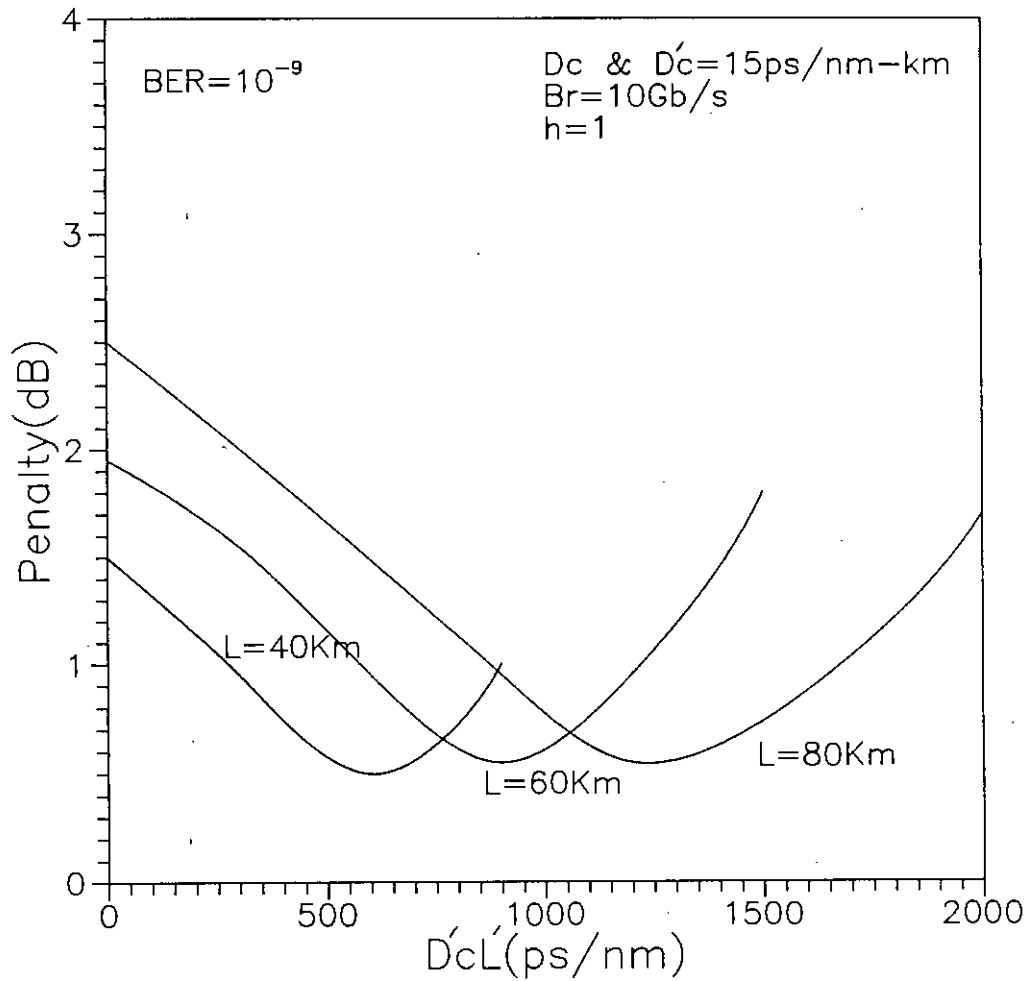


Fig. 3.5 Plots of penalty in signal power due to GVD in a point to point optical CPFSK link with lump compensation at $\text{BER}=10^{-9}$ versus $D'_c L'$ with fibre length $L=40, 60, 80$ km and modulation index $h=1$.

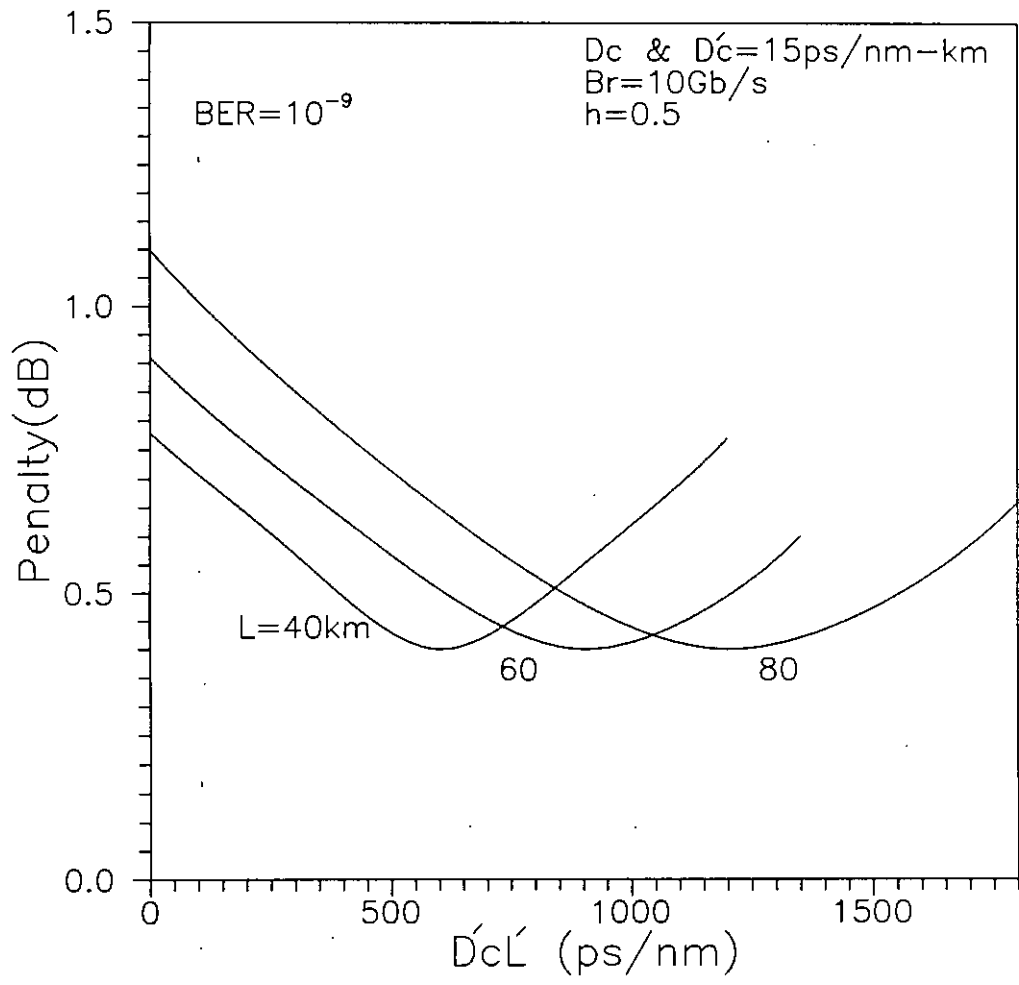


Fig. 3.6 Plots of penalty in signal power due to GVD in a point to point optical CPFSK link with lump compensation at $BER=10^{-9}$ versus $D'_c L'$ with fibre length $L=40, 60, 80$ km and modulation index $h=0.5$.

chromatic dispersion with lump compensation scheme is shown in Fig. 3.6 for a modulation index $h = 0.5$. From this figure it is evident that penalty is lower for $h=0.5$ than that for $h=1$. It is observed that the system suffers less penalty in signal power at decreased value of modulation index. This is due to the fact that the FSK spectrum becomes broadened at higher modulation index and the effect of dispersion is more prominent at increased bandwidth of the signal spectrum.

The bit error rate (BER) performance of the point to point optical link with even compensation is depicted in Fig. 3.7 . The dispersive fibre length is taken as $L = 100\text{km}$, compensator length in each section $L'_a = 10\text{km}$, fibre length in each section $L_a = L / N$, where N is the number of sections and BER performance is plotted for $N = 1, 2, 3, 4, 5$. As the number of sections in the even compensation scheme increases, the required signal power decreases for a given value of BER. This is due to the fact that as the number of fibre section increases the effect of dispersion becomes less dominant as the length of fibre in each section decreases. The BER performance for same parameters with $L'_a = 20\text{km}$ and $L'_a = 40\text{km}$ are also provided in Fig. 3.8 and Fig. 3.9 respectively.

The plots of penalty in signal power due to fibre chromatic dispersion with even compensation scheme at $\text{BER}=10^{-9}$ for modulation index $h = 1$ is depicted in Fig. 3.10. The penalty is plotted as a function of number of fibre sections with compensator length L'_a as a parameter. The penalties are calculated from Fig. 3.7 through Fig. 3.9. It is found that penalty decreases as the number of section increases for lower value of compensator length. For higher values of compensator length penalty decreases upto certain number of section then again increases. This is a minimum penalty which is found to be less for lower compensator length with higher number of sections. This is due to lower value

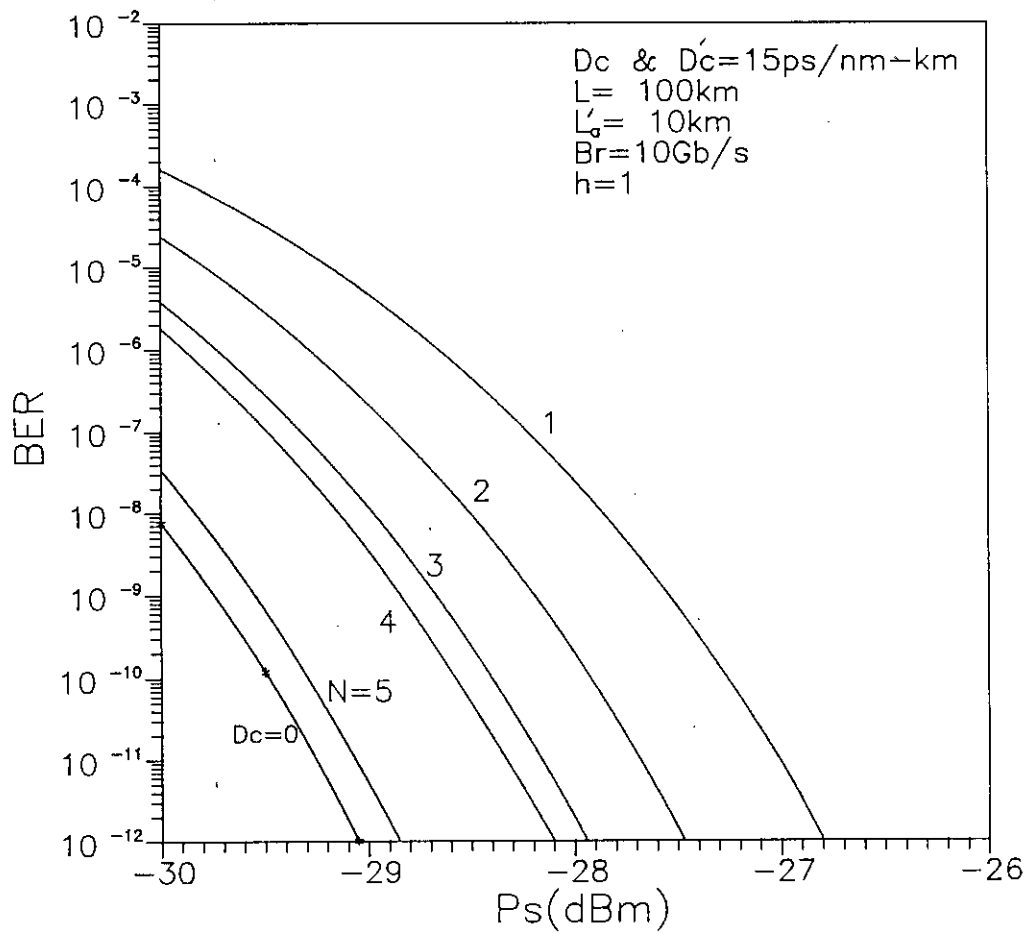


Fig. 3.7 The bit error rate (BER) performance of a point to point optical link with even compensation for direct detection FSK system at a bit rate of 10 Gb/s with dispersion coefficient $D_c \text{ \& } D'_c = 15 \text{ ps/nm-km}$, fibre length $L = 100 \text{ km}$, compensator length in each section $L'_a = 10 \text{ km}$, modulation index $h = 1$ at an wavelength of 1550 nm, for several number of fibre sections N .

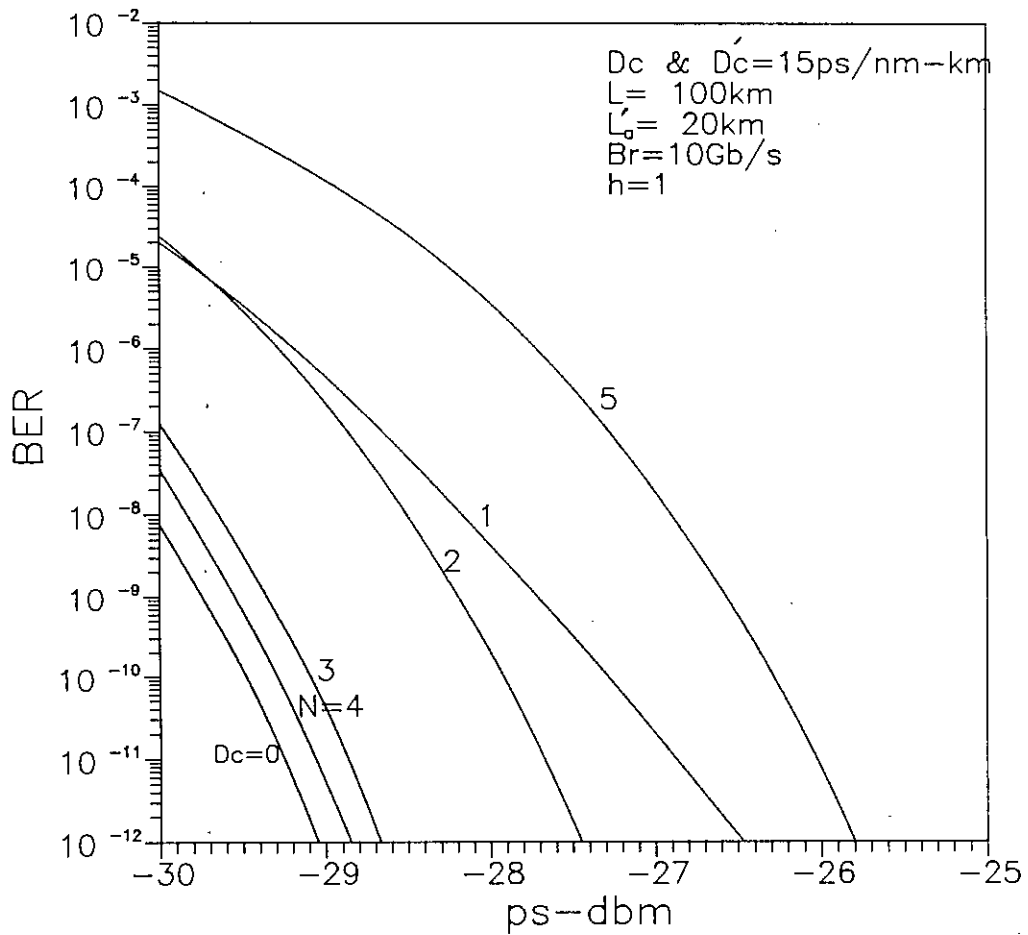


Fig. 3.8 The bit error rate (BER) performance of a point to point optical link with even compensation for direct detection FSK system at a bit rate of 10 Gb/s with dispersion coefficient $D_c \ \& \ D'_c = 15 \text{ ps/nm-km}$ fibre length $L = 100 \text{ km}$, compensator length in each section $L'_a = 20 \text{ km}$, modulation index $h = 1$ at an wavelength of 1550 nm, for several number of fibre sections N .

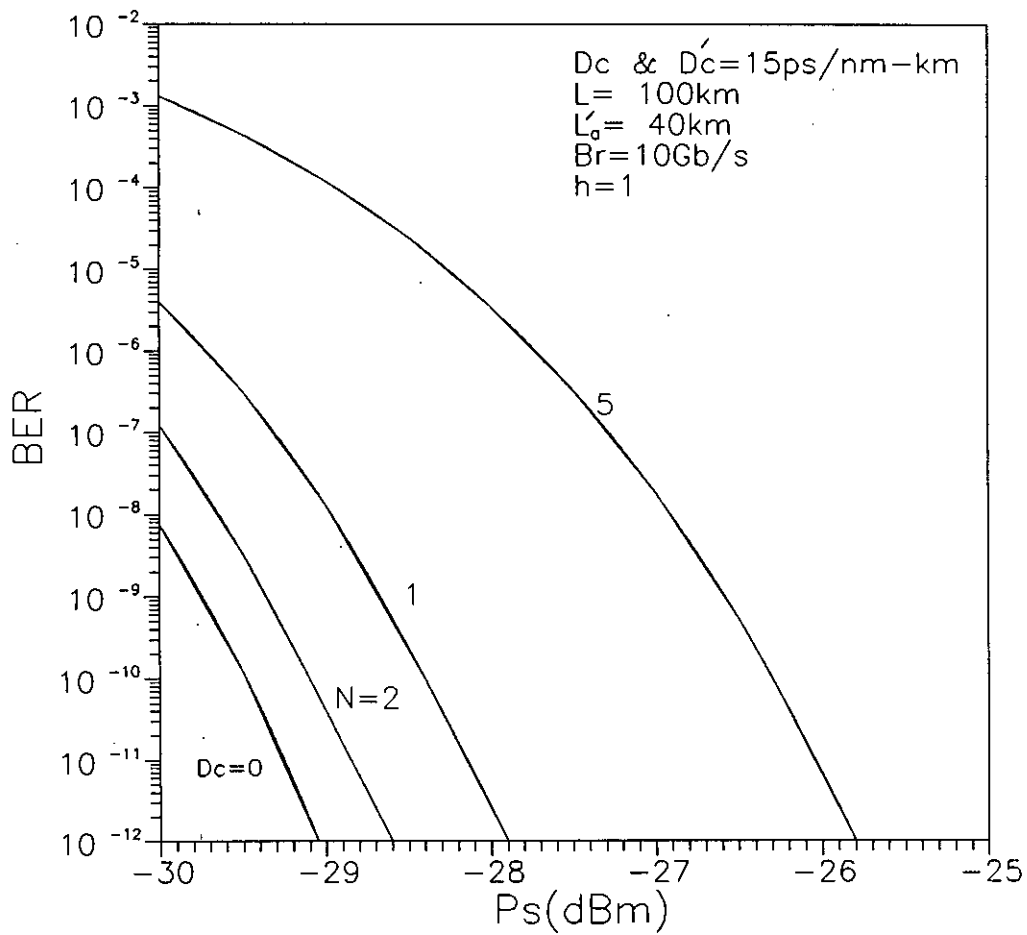


Fig. 3.9 The bit error rate (BER) performance of a point to point optical link with even compensation for direct detection FSK system at a bit rate of 10 Gb/s with dispersion coefficient $D_c \text{ \& } D'_c = 15 \text{ ps/nm-km}$, fibre length $L = 100 \text{ km}$, compensator length in each section $L'_a = 40 \text{ km}$, modulation index $h = 1$ at an wavelength of 1550 nm, for several number of fibre sections N .

of ASE noise corresponding to lower value of amplifier gain.

The plots of penalty in signal power due to fibre chromatic dispersion with even compensation scheme at $BER=10^{-9}$ for total fibre length $L=300\text{km}$ with modulation index $h = 1$ is depicted in Fig. 3.11. Observations found from this plot are similar to that observed in Fig. 3.10.

The plots of minimum penalty in signal power as a function of number of fibre sections is depicted in Fig. 3.12. The penalty values are obtained from Fig. 3.10 and Fig. 3.11. for two fibre length $L = 100\text{km}$ and 300km . It is found that penalty is less for smaller length of the dispersive fibre.

Including the effect of self-phase-modulation (SPM), the bit error rate (BER) performance of point to point optical link with lump compensation is depicted in Fig. 3.13 in presence of ASE noise due to the cascaded EDFAs and receiver noises. The BER values are obtained for a fibre length $L=50\text{km}$ with input power $P_{in}=0\text{dBm}$ and different values of compensator length i.e. $L' = 10, 30, 50, 70$ and 90km for a modulation index $h = 1$. It is found from this figure that for a given input power the BER decreases with increase in compensator length L'_a upto full compensation and again increases with increased compensator length.

Similar performance results including the effect of SPM are depicted in Fig. 3.14 and Fig. 3.15 for two different input power levels, viz. $P_{in}=5\text{dBm}$ and $P_{in}=8\text{dBm}$ respectively. Comparison of the results show that BER is higher in spite of full compensation in case of $P_{in}=8\text{dBm}$. This is because the effect of SPM is more predominate at higher input power level.

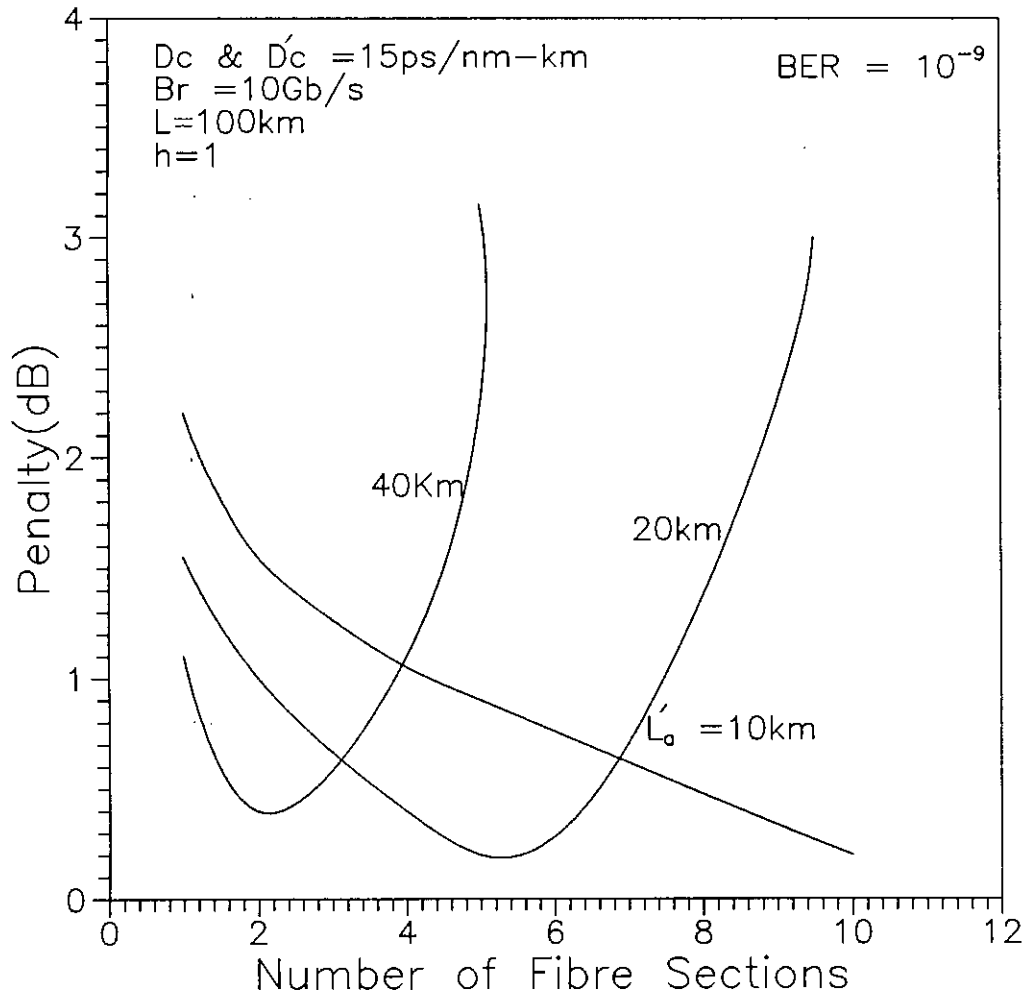


Fig. 3.10 Plots of penalty in signal power due to GVD in a point to point optical link with even compensation at of $\text{BER} = 10^{-9}$ versus number of fibre section with fibre length $L = 100 \text{ km}$ compensator length in each section $L'_a = 10, 20, 40 \text{ km}$ and modulation index $h = 1$.

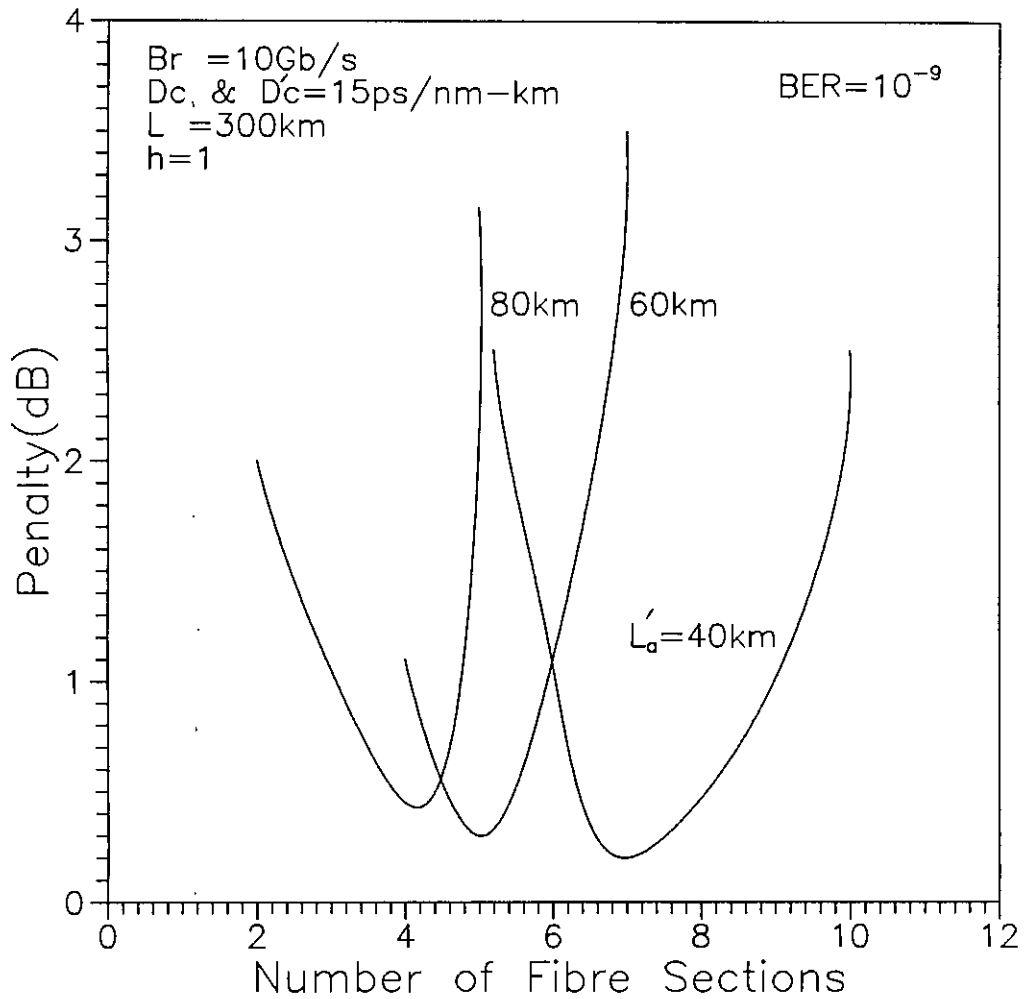


Fig. 3.11 Plots of penalty in signal power due to GVD in a point to point optical link with even compensation at of $\text{BER} = 10^{-9}$ versus number of fibre section with fibre length $L = 300\text{ km}$ compensator length in each section $L'_a = 40, 60, 80\text{ km}$ and modulation index $h = 1$.

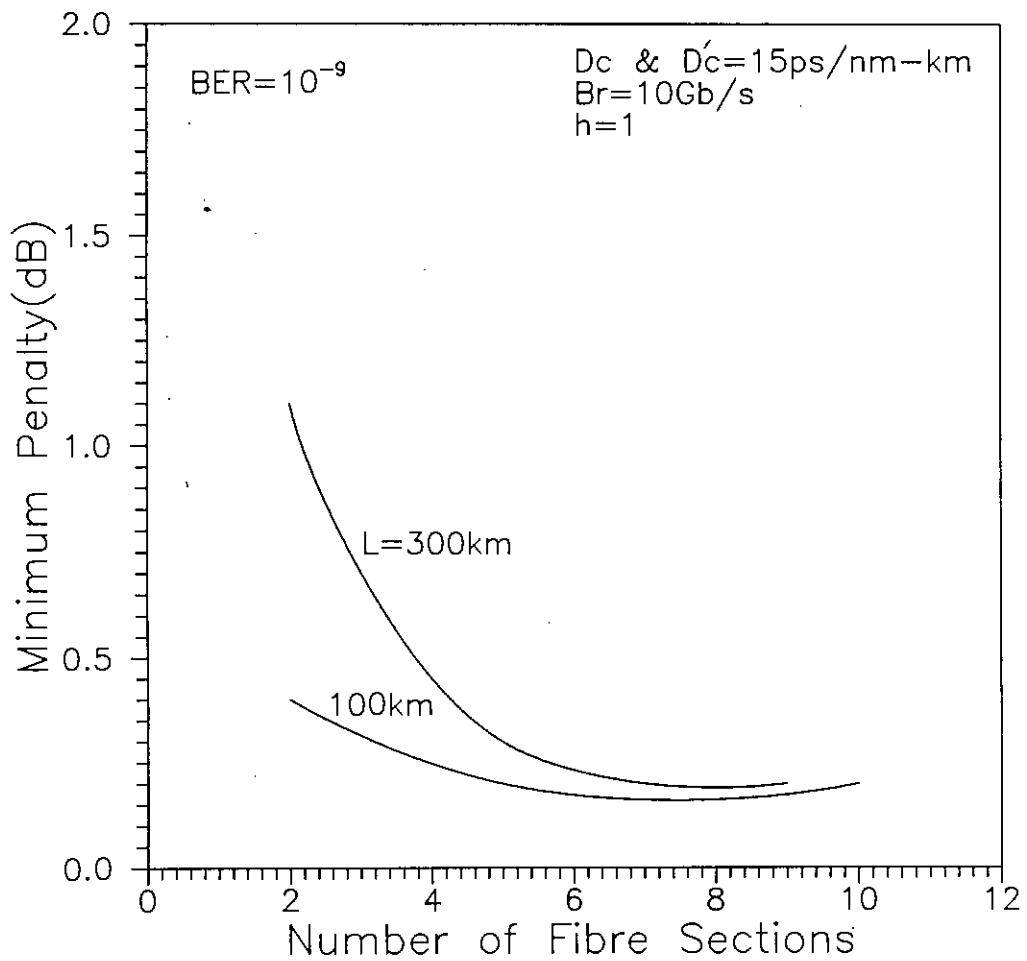


Fig. 3.12 Plots of minimum penalty in signal power of a point to point optical link with even compensation at BER=10⁻⁹ versus number of fibre section with fibre length L=100km and 300km and modulation index h=1.

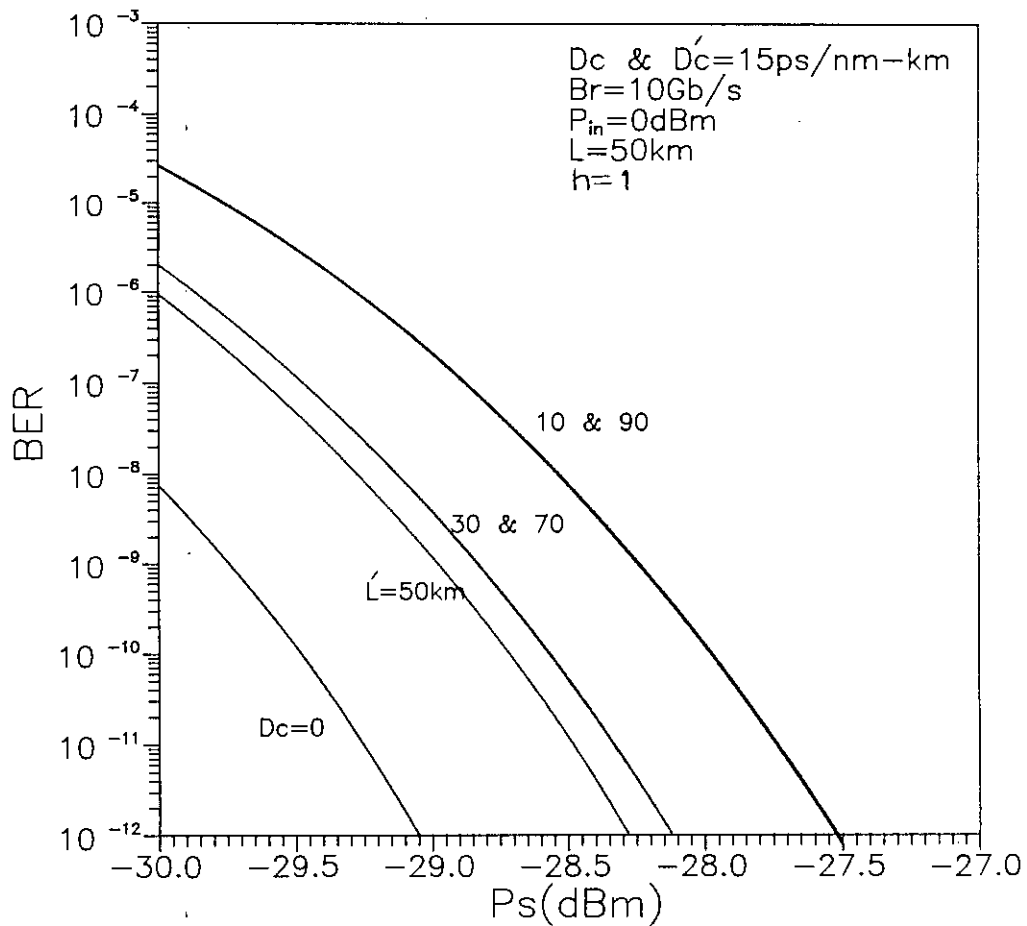


Fig. 3.13 The bit error rate (BER) performance of a point to point optical link with lump compensation in presence of GVD and SPM for direct detection FSK system at a bit rate of 10 Gb/s with dispersion coefficient $D_c \text{ \& } D'_c = 15 \text{ ps/nm-km}$, fibre length $L = 50 \text{ km}$, $P_{in} = 0 \text{ dBm}$ at an wavelength of 1550 nm and modulation index $h = 1$ for several values of compensator length L' .

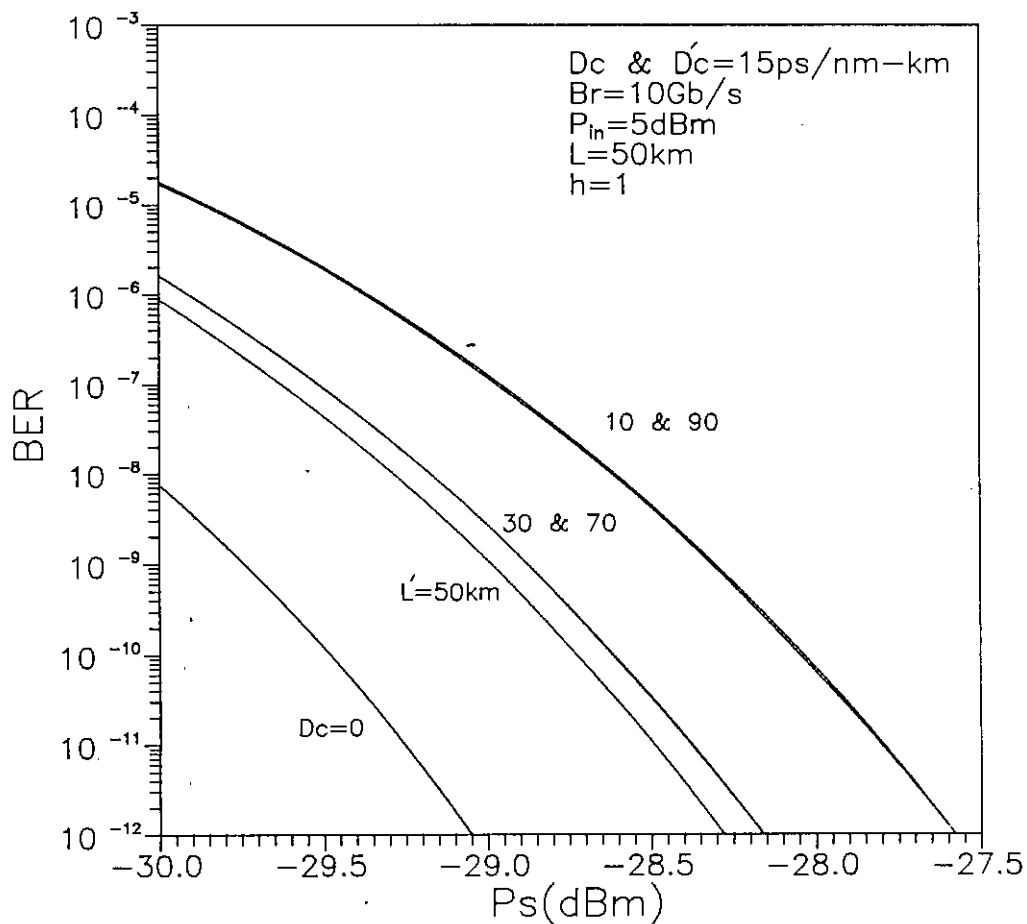


Fig. 3.14 The bit error rate (BER) performance of a point to point optical link with lump compensation in presence of GVD and SPM for direct detection FSK system at a bit rate of 10 Gb/s with dispersion coefficient $D_c \text{ \& } D'_c = 15 \text{ ps/nm-km}$, fibre length $L = 50 \text{ km}$, $P_{in} = 5 \text{ dBm}$ at an wavelength of 1550 nm and modulation index $h = 1$ for several values of compensator length L' .

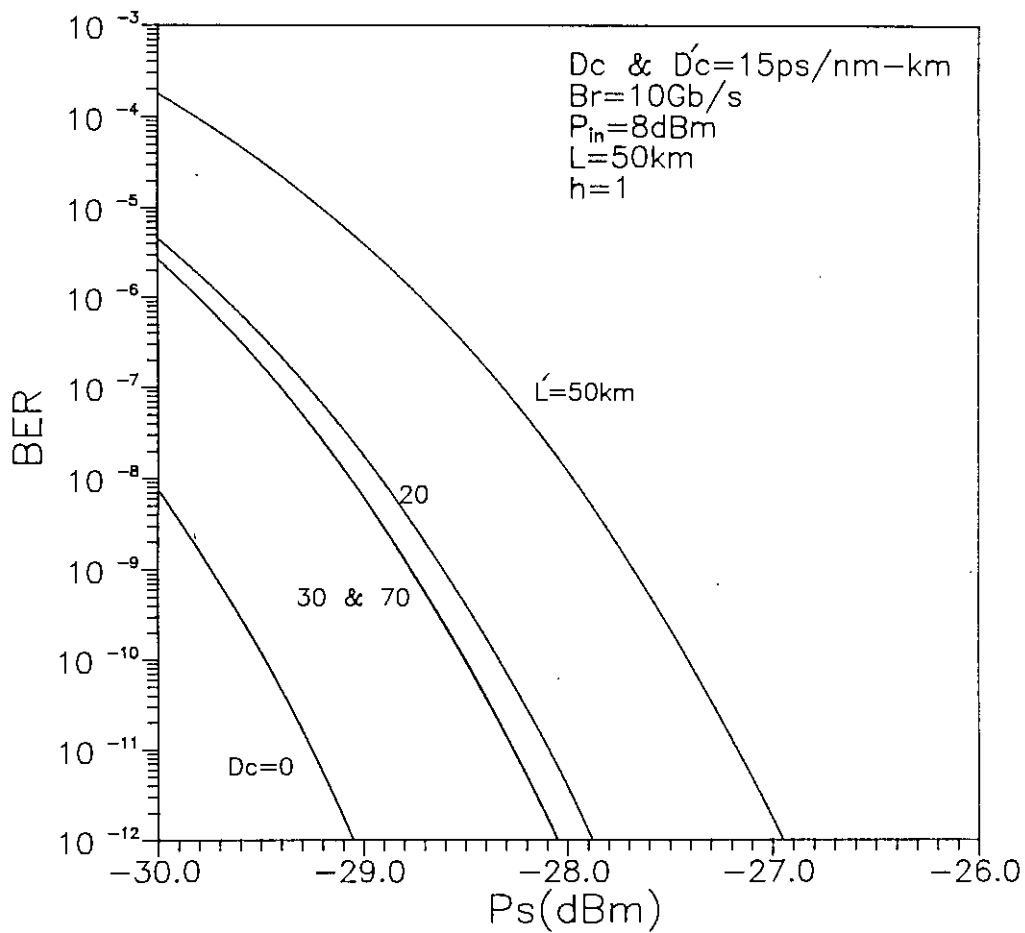


Fig. 3.15 The bit error rate (BER) performance of a point to point optical link with lump compensation in presence of GVD and SPM for direct detection FSK system at a bit rate of 10 Gb/s with dispersion coefficient $D_c \text{ \& } D'_c = 15 \text{ ps/nm-km}$, fibre length $L = 50 \text{ km}$, $P_{in} = 8 \text{ dBm}$ at an wavelength of 1550 nm and modulation index $h = 1$ for several values of compensator length L' .

The plots of penalty in signal power due to the combined effect of SPM and GVD with lump compensation scheme at $BER=10^{-9}$ for modulation index $h = 1$ is depicted in Fig. 3.16. The penalty is plotted as a function of compensating fibre length L' with input power P_{in} as a parameter. The penalties are determined from Fig. 3.13 through Fig. 3.15. It is found that penalty decreases with increase in compensator length and again increases after attaining a minimum penalty which corresponds to full dispersion compensation. At higher input power level, the minimum penalty corresponding to full GVD compensation occurs at a small value of the compensating fibre length. This is due to the fact that the effect of SPM opposes the effect of GVD and the effect of SPM is more dominant at higher input power. Thus after full compensation of GVD, effect of SPM increases more rapidly with compensator length. However, as the compensator length increases, the effect of GVD in the compensating fibre increases and tends to nullify the effect of SPM and consequently the penalty after attaining a peak gradually decreases to its minimum value at some higher value of compensator length. It is also observed that the peak value of the penalty is higher for higher input power level due to enhanced effect of SPM. Similar behavior is also observed in Fig. 3.17 for $h=0.5$.

The plot of penalty in signal power due to GVD and SPM is depicted in Fig. 3.18. The penalty in signal power is plotted as a function of input power P_{in} (dBm) with compensator length as a parameter. It is depicted from the figure that penalty increases rapidly when the effect of GVD is fully compensated and the penalty is only due to SPM. At any other value of the compensator length GVD and SPM works in opposite and the penalty increases gradually with fibre length.

Similar observations are also found in the plot of penalty in signal power due to GVD and SPM for $h=0.5$ is shown in Fig. 3.19. Comparing Fig. 3.18 and Fig.

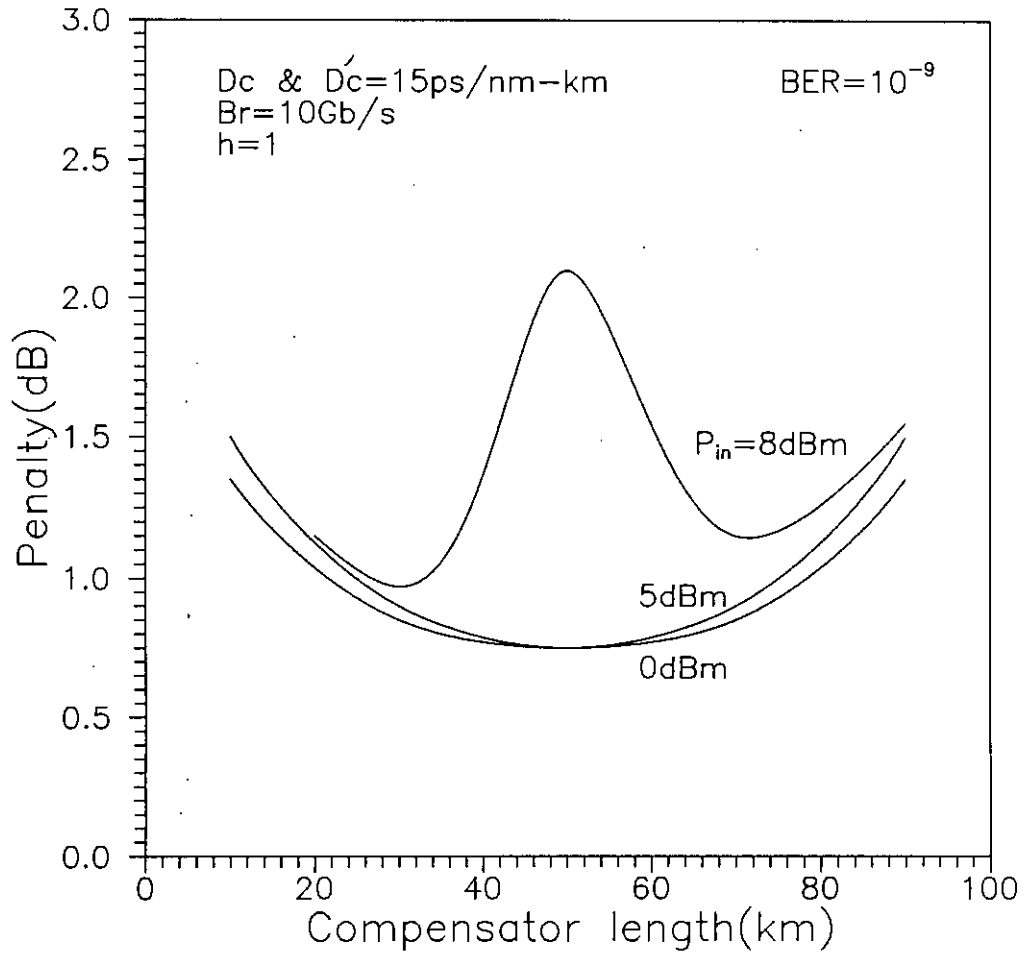


Fig. 3.16 Plots of penalty in signal power due to GVD and SPM in a point to point optical link with lump compensation at of $BER=10^{-9}$ versus compensator length L' with dispersion coefficient $D_c \text{ \& } D'_c = 15 \text{ ps/nm-km}$, fibre length $L=50 \text{ km}$, $P_{in} = 0, 5, 8 \text{ dBm}$ and modulation index $h=1$.

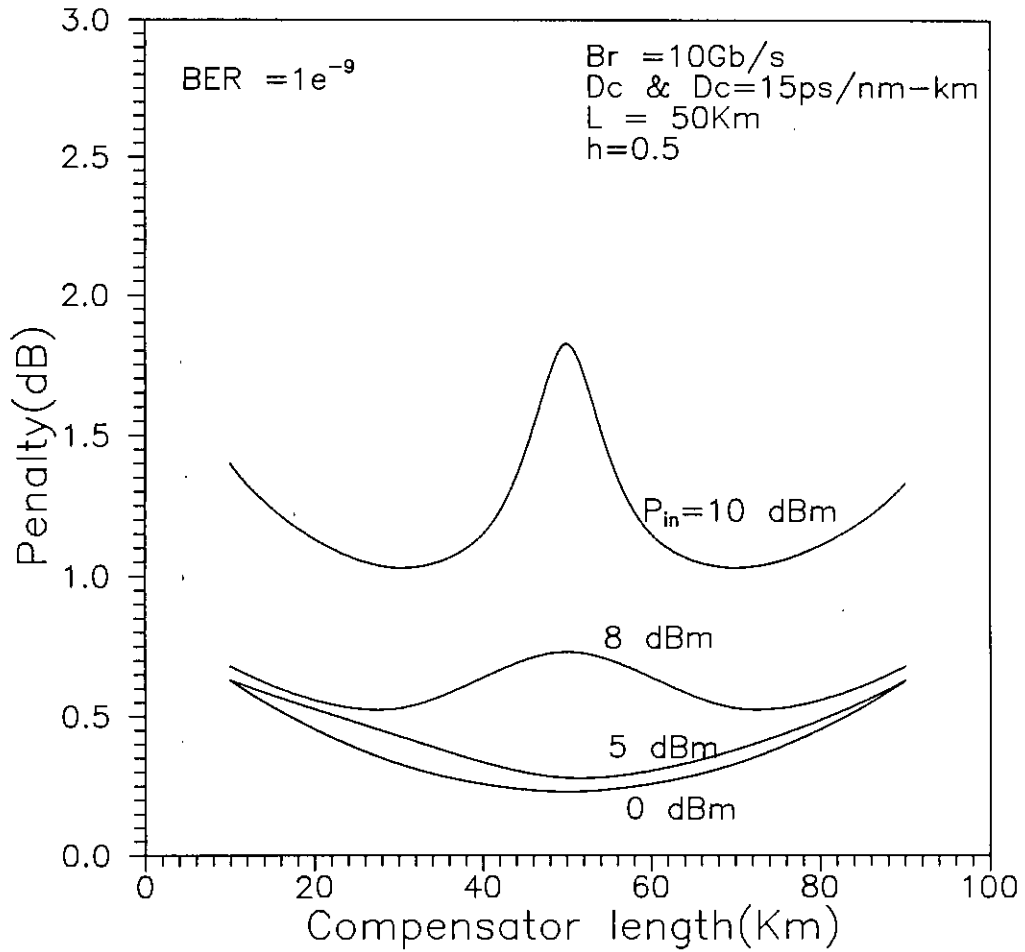


Fig. 3.17 Plots of penalty in signal power due to GVD and SPM in a point to point optical link with lump compensation at of $BER=10^{-9}$ versus compensator length L' with dispersion coefficient D_c & $D_c' = 15\text{ps/nm-km}$, fibre length $L=50\text{km}$, $P_{in} = 0, 5, 8$ dBm and modulation index $h=0.5$.

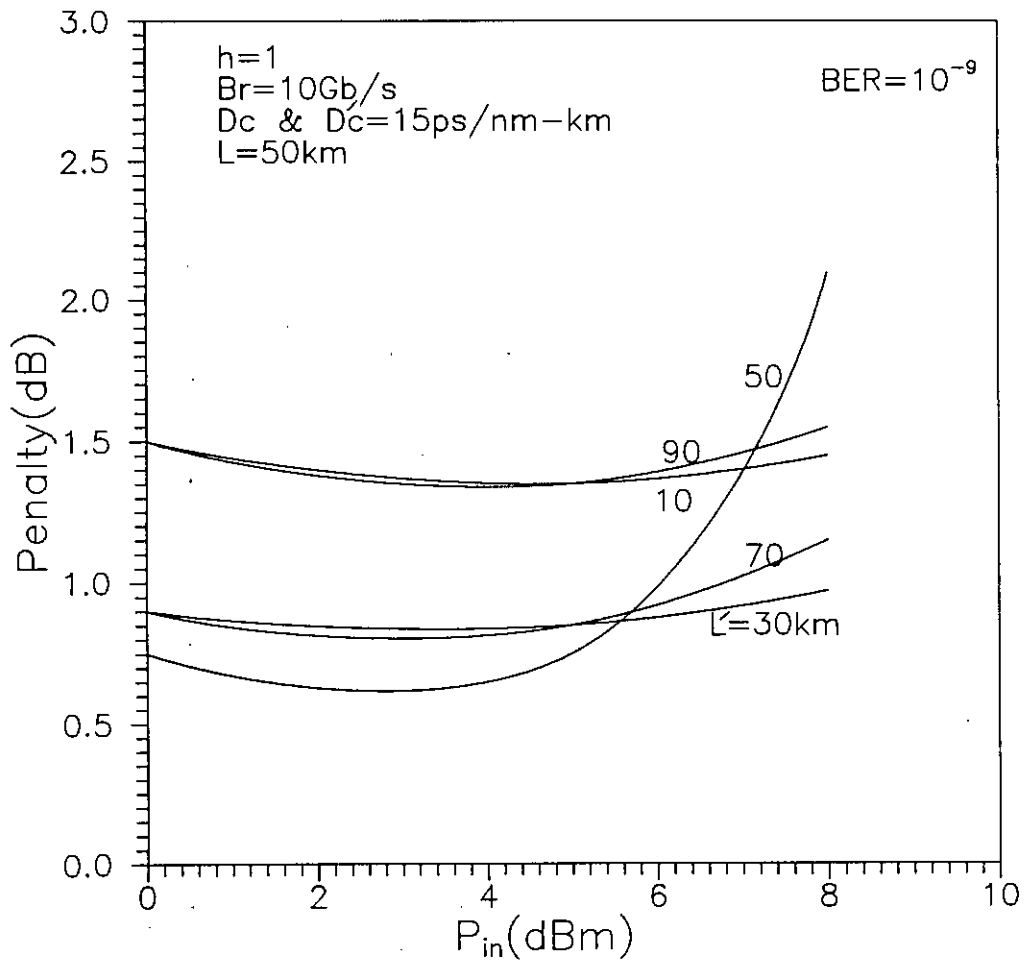


Fig. 3.18 Plots of penalty in signal power due to GVD and SPM in a point to point optical link with lump compensation at of $BER=10^{-9}$ versus fibre input power for fibre length $L=50\text{km}$ and modulation index $h=1$ with compensator length as parameter.

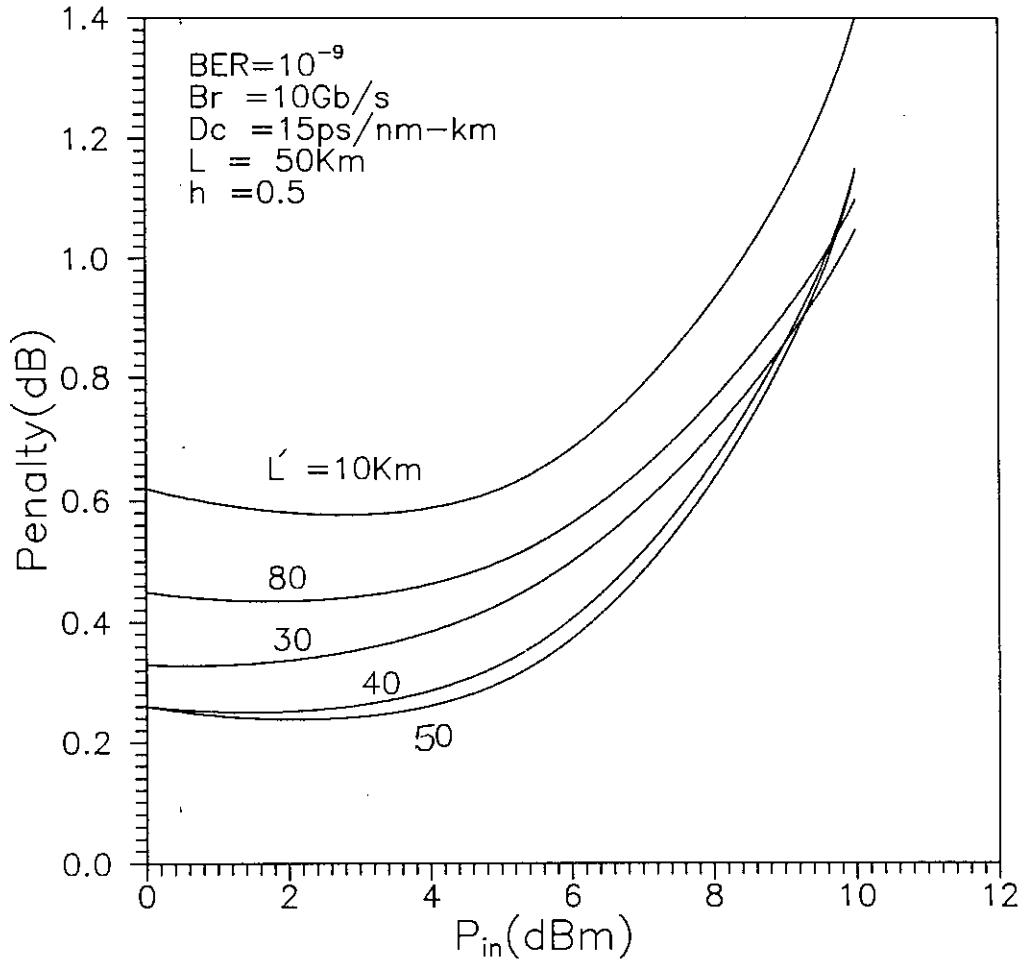


Fig. 3.19 Plots of penalty in signal power due to GVD and SPM in a point to point optical link with lump compensation at $BER=10^{-9}$ versus fibre input power for fibre length $L=50\text{km}$ and modulation index $h=0.5$ with compensator length as parameter.

3.19 it is found that for $h=0.5$ penalty increases less rapidly with input signal than that of for $h=1$. This may be due to the fact that the FSK spectrum becomes broadened at higher modulation index and the effect of SPM is more prominent at increased bandwidth of the signal spectrum.

The bit error rate (BER) performance of AMI coded optical CPFSK system without compensation is depicted in Fig. 3.20 in the presence of GVD, accumulated ASE and receiver noise. The BER values are obtained for different fibre length L and for a modulation index $h = 1$. It is observed that required signal power for a given BER increases with the increase in fibre length. Similar performance results are plotted for AMI encoded bit pattern with $h=0.5$ in Fig. 3.21.

The penalty due to GVD for AMI coded CPFSK system at $BER=10^{-9}$ is plotted in Fig. 3.22 for $h=0.5$ and $h=1$. It is observed that penalty is less for $h=0.5$ and increases more sharply with increasing fibre length for $h=1$.

The bit error rate (BER) performance results for DM coded CPFSK system without compensation is depicted for $h=1$ and $h=0.5$ in Fig. 3.23 and Fig. 3.24 respectively with fibre length as a parameter. The plot of penalty at $BER=10^{-9}$ is shown in Fig. 3.25 for $h=0.5$ and $h=1$. The penalty reduces with increasing value of L and attains a minimum value and then again increases. However, the minimum penalty is less for $h=1$ than for $h=0.5$.

The bit error rate (BER) performance results for MC coded CPFSK system without compensation is depicted in Fig. 3.26. It is observed that required signal power for a given BER first decreases with increase of fibre length then again increases. Similar BER performance results for $h=0.5$ is depicted in Fig. 3.27. The penalty is found to be higher for $h=1$ compared to $h=0.5$. The penalty

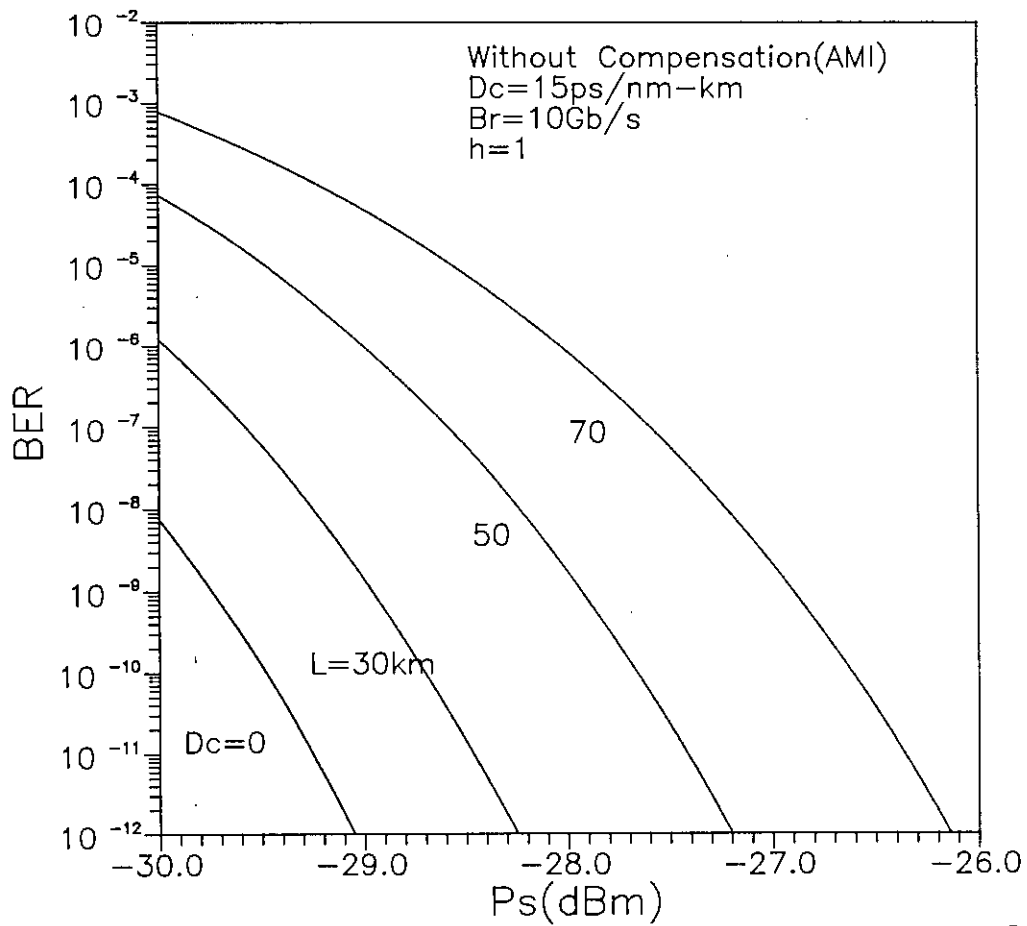


Fig. 3.20 The bit error rate (BER) performance of an optical CPFSK link without any compensation with AMI line coded bit pattern at a bit rate of 10 of Gb/s with fibre chromatic dispersion $D_c = 15 \text{ ps/nm-km}$, modulation index $h = 1$ at an wavelength of 1550 nm, with fibre length L as parameter.

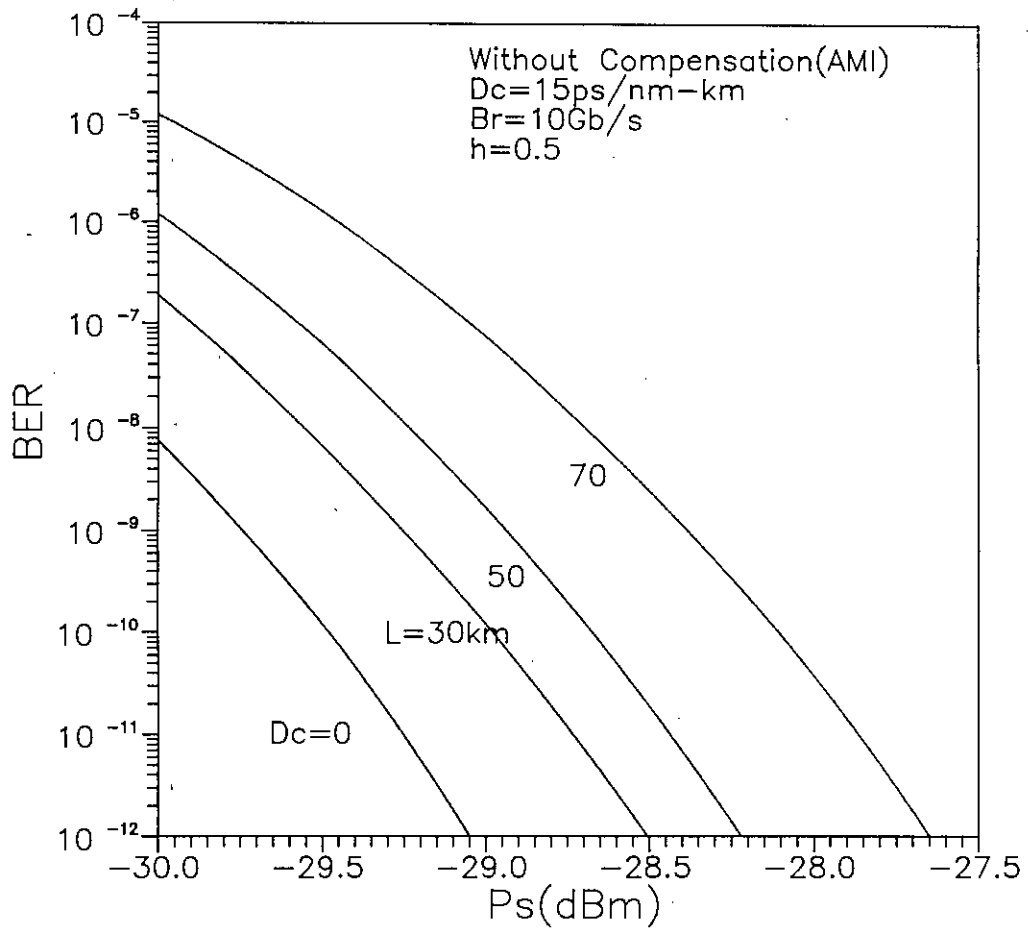


Fig. 3.21 The bit error rate (BER) performance of an optical CPFSK link without any compensation with AMI line coded bit pattern at a bit rate of 10 of Gb/s with fibre chromatic dispersion $D_c = 15 \text{ ps/nm-km}$, modulation index $h = 0.5$ at an wavelength of 1550 nm, with fibre length L as parameter.

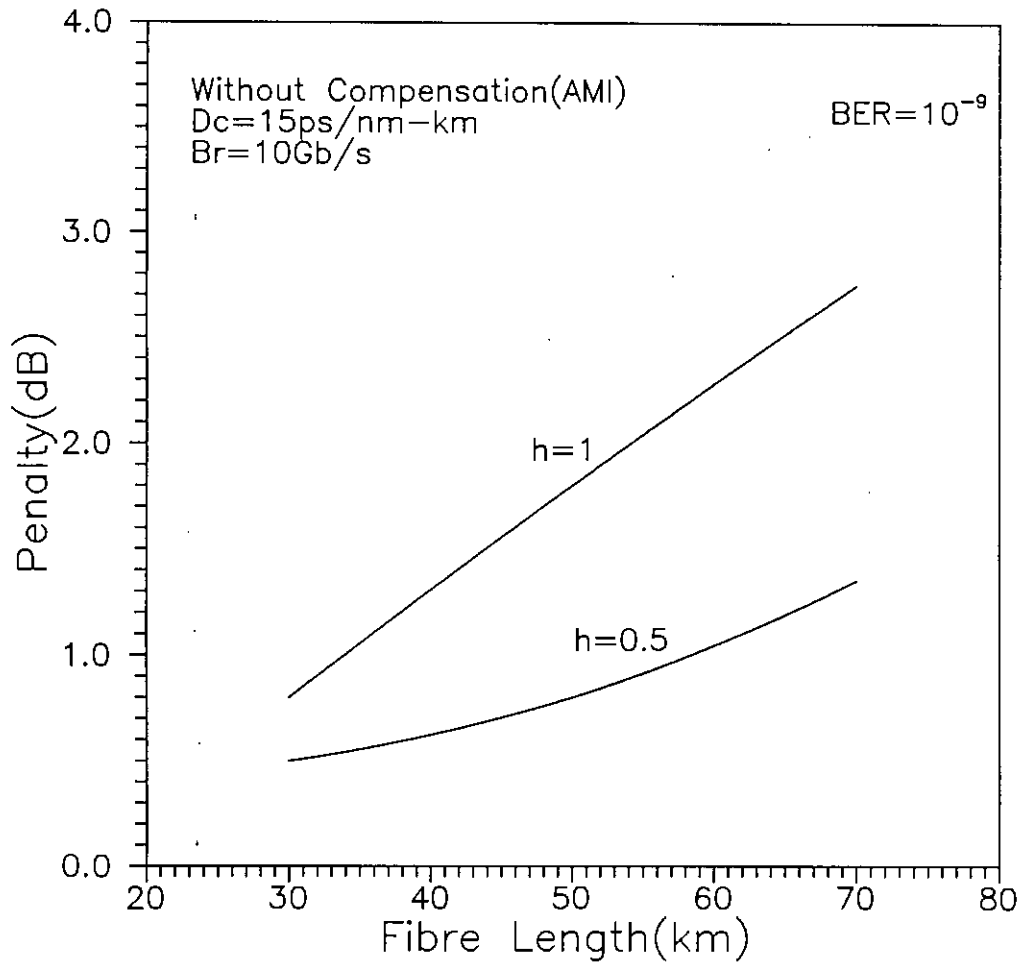


Fig. 3.22 Plots of penalty in signal power due to GVD in a point to point optical CPFSK link without any compensation versus fibre length with AMI line coded bit pattern at a bit rate of 10 Gb/s at $\text{BER} = 10^{-9}$ with modulation index h as parameter.

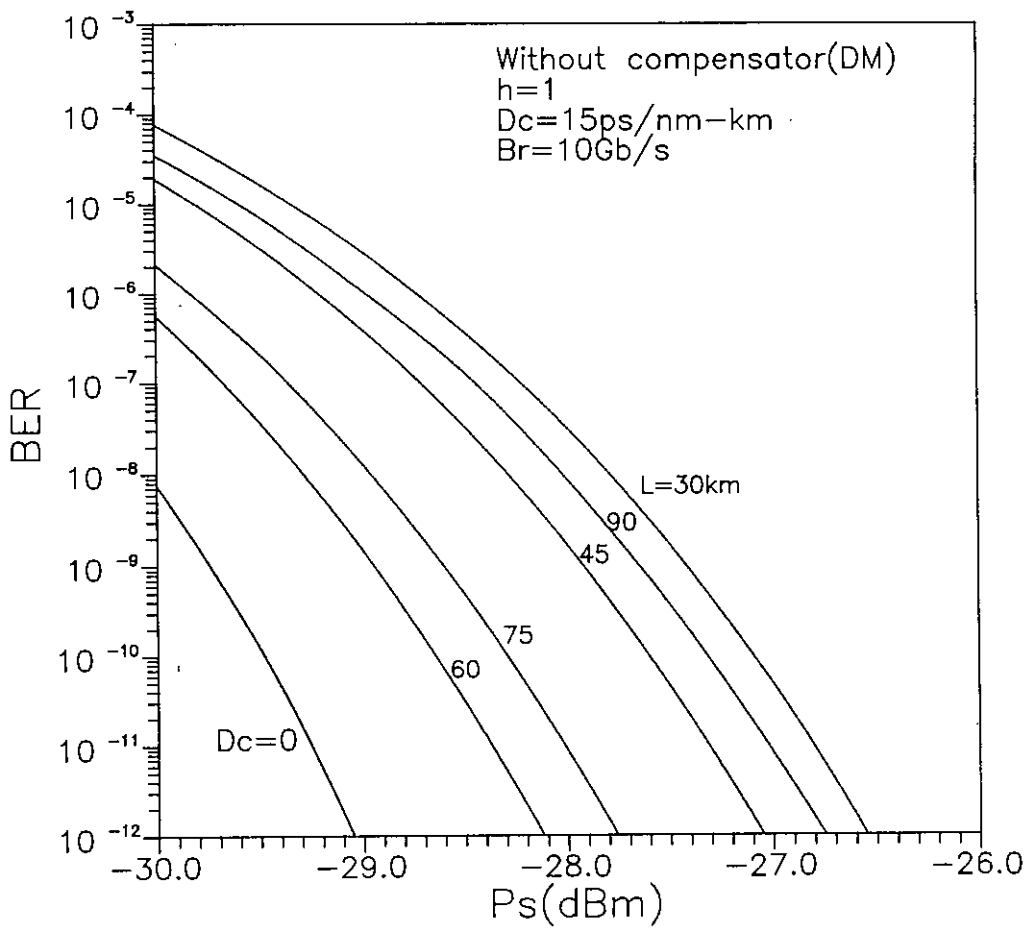


Fig. 3.23 The bit error rate (BER) performance of an optical CPFSK link without any compensation with DM line coded bit pattern at a bit rate of 10 of Gb/s with fibre chromatic dispersion $D_c=15\text{ps/nm-km}$, modulation index $h=1$ at an wavelength of 1550 nm, with fibre length L as parameter.

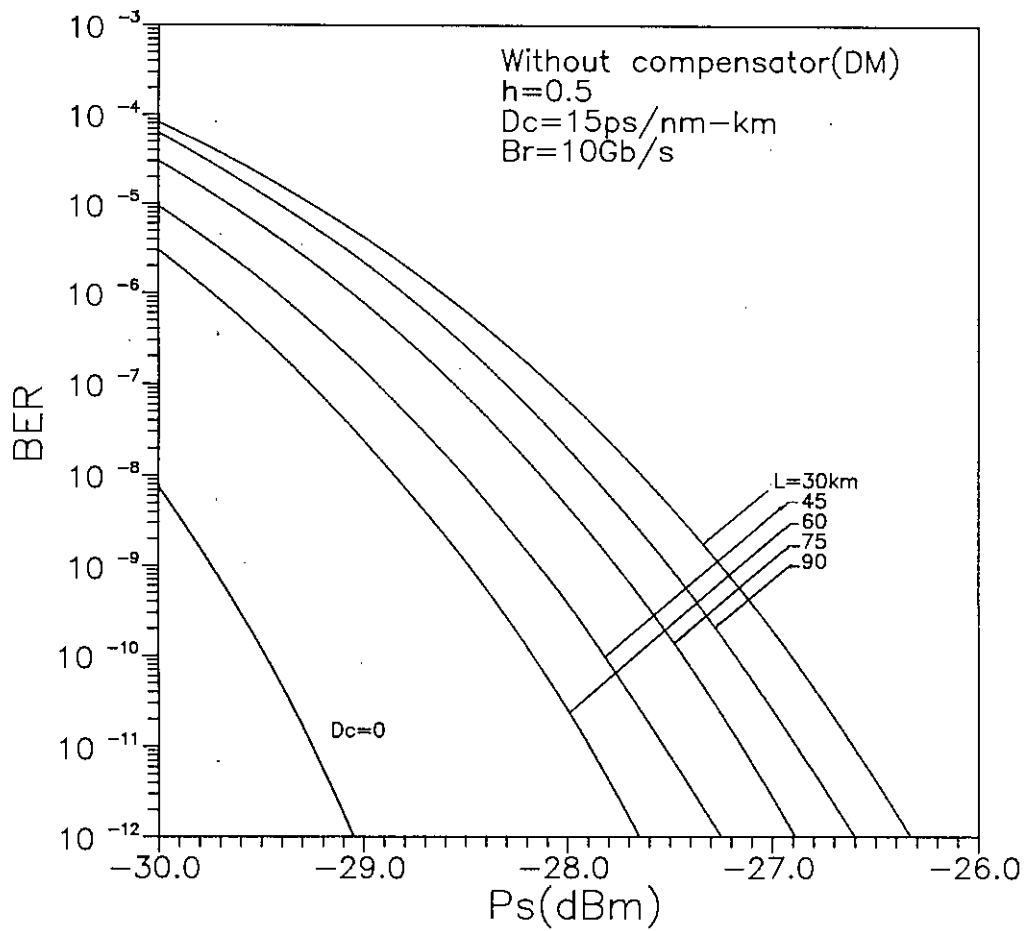


Fig. 3.24 The bit error rate (BER) performance of an optical CPFSK link without any compensation with AMI line coded bit pattern at a bit rate of 10 of Gb/s with fibre chromatic dispersion $D_c=15\text{ps/nm-km}$, modulation index $h=0.5$ at an wavelength of 1550 nm, with fibre length L as parameter.

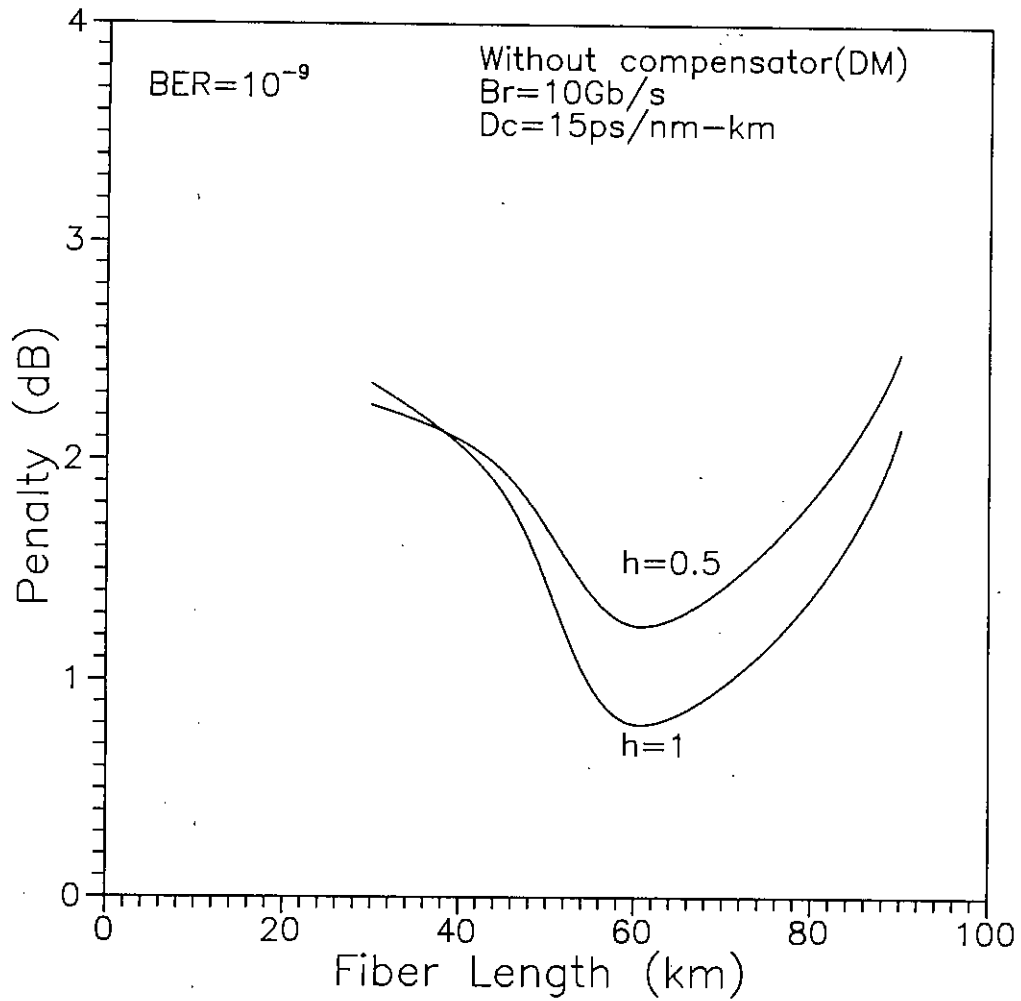


Fig. 3.25 Plots of penalty in signal power due to GVD in a point to point optical CPFSK link without any compensation versus fibre length with DM line coded bit pattern at a bit rate of 10 Gb/s at $BER=10^{-9}$ with modulation index h as parameter.

92602

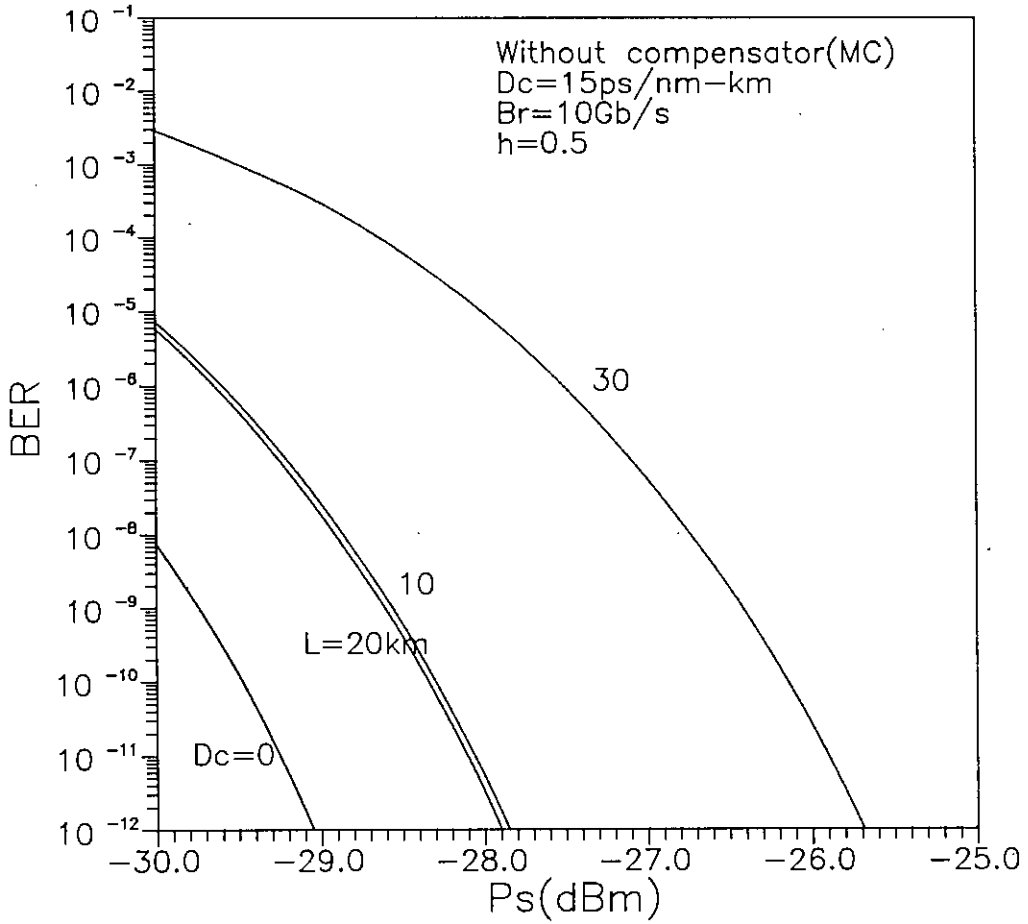


Fig. 3.26 The bit error rate (BER) performance of an optical CPFSK link without any compensation with MC line coded bit pattern at a bit rate of 10 of Gb/s with fibre chromatic dispersion $D_c=15\text{ps/nm-km}$, modulation index $h=1$ at an wavelength of 1550 nm, with fibre length L as parameter.

in signal power is plotted in Fig. 3.28 as a function of fibre length L with modulation index h as a parameter. It is depicted from the figure that penalty first decrease then again increases.

Finally, plots of the minimum penalty in signal power for three linecoding systems i.e. AMI, DM, MC with full compensation are depicted in Fig. 3.29 considering only the effect of fibre chromatic dispersion as a function of fibre length L . The penalties are constant since signals are fully compensated for any fibre length. The minimum value corresponding to $h=0.5$ for MC encoding is 0.38dB. The next higher value is for AMI which is 0.4dB and DM shows a higher penalty of 0.6dB. Thus, among the three linecoding schemes, least penalty occurs in case of MC compared to the other two.

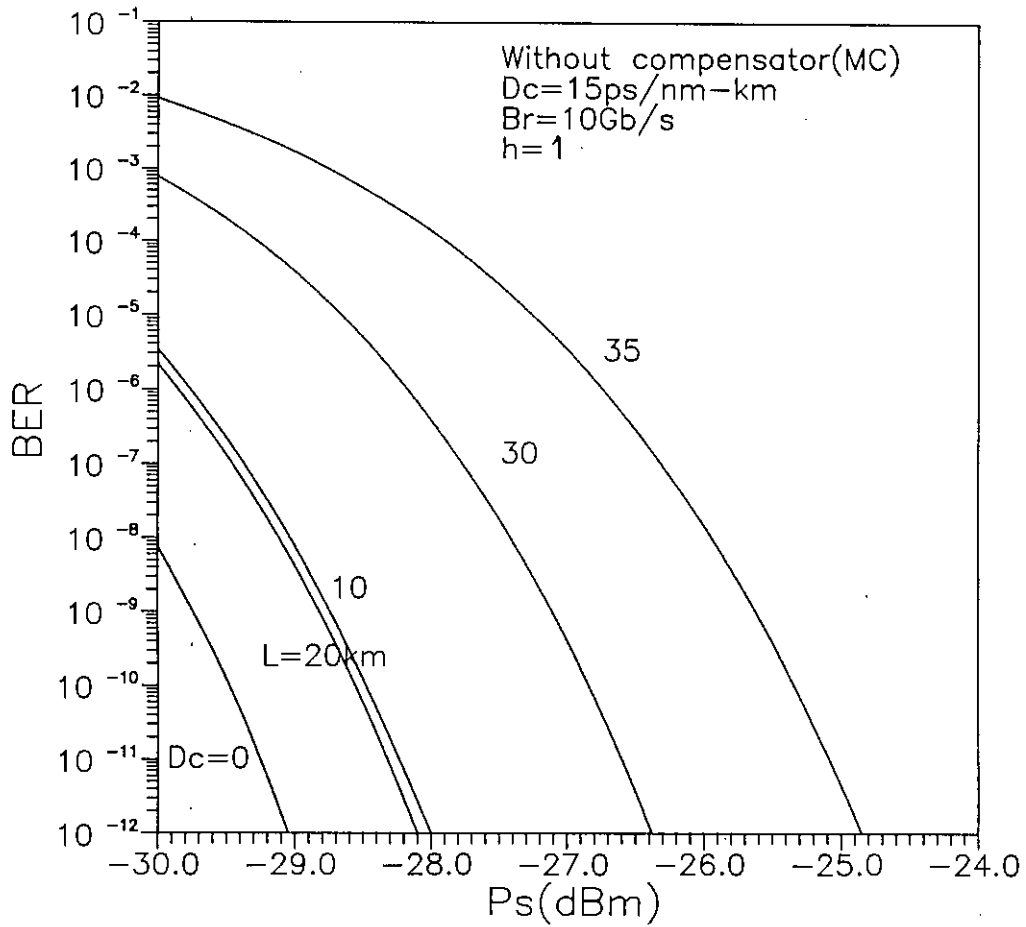


Fig. 3.27 The bit error rate (BER) performance of an optical CPFSK link without any compensation with MC line coded bit pattern at a bit rate of 10 of Gb/s with fibre chromatic dispersion $D_c=15\text{ps/nm-km}$, modulation index $h=0.5$ at an wavelength of 1550 nm, with fibre length L as parameter.

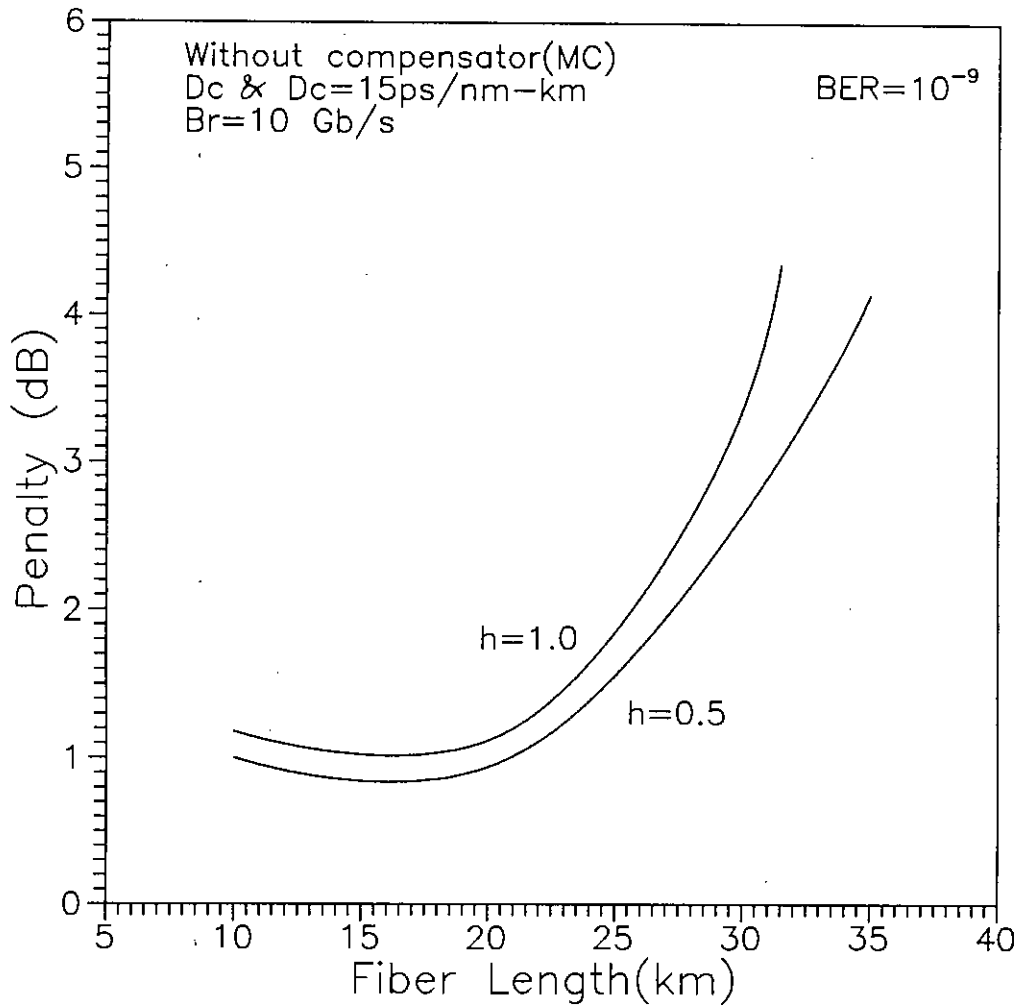


Fig. 3.28 Plots of penalty in signal power due to GVD in a point to point optical CPFSK link without any compensation versus fibre length with MC line coded bit pattern at a bit rate of 10 Gb/s at $BER=10^{-9}$ with modulation index h as parameter.

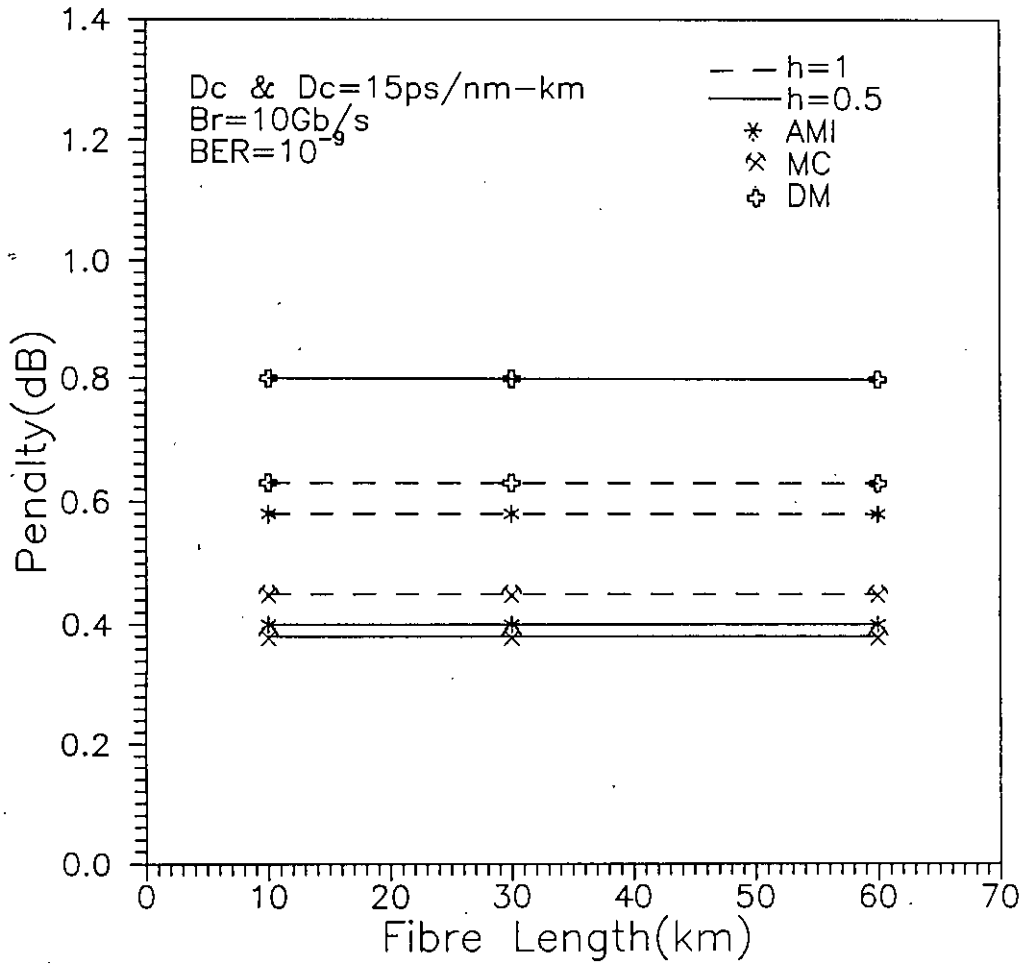


Fig. 3.29 Plots of penalty in signal power due to GVD in an optical direct detection CPFSK system with full compensation versus fibre length for different line-coding data pattern at a bit rate of 10 Gb/s at $BER=10^{-9}$ with modulation index h as parameter.

CHAPTER-4

CONCLUSIONS AND SUGGESTION FOR FUTURE WORKS

4.1 Conclusions

A theoretical analysis is carried out to evaluate the efficacy of two different dispersion compensation schemes, viz. lump compensation and even compensation to minimize the effect of group velocity dispersion (GVD) on the performance of an optical CPFSK point to point transmission system using MZI based direct detection receiver. The analysis is extended to linecoded CPFSK system with three line-coding schemes, viz. AMI, DM, MC. Following the theoretical analysis the performance results are evaluated at a bit rate of 10Gb/s. The analysis is also carried out to find out the impact of SPM on the system performance with GVD compensation.

From the computed results it is observed that the effect of GVD can be compensated by using the above two different compensation schemes. The penalty suffered by the system due to GVD and accumulated ASE can be reduced to a minimum value corresponding to an optimum length of the compensating fibre. For example, the penalty for $h=1$ and $L=40\text{km}$ is 1.5dB when there is no compensation. When lump compensation is used the minimum penalty is found to be 0.5dB. Further, when modulation index is reduced to 0.5, the above penalty values are found to be 0.8 dB and 0.4 dB respectively. When even compensation is used the minimum penalty is found to be 0.4 dB. Further, when modulation index is reduced to 0.5, the above penalty value is found to be

0.25 dB. From these values it is found that even compensation can compensate more effectively than lump compensation. Further, the lump compensation requires a larger length of compensator for long-distance transmission. In even compensation it is also observed that penalty decreases with increased number of fibre sections. But it is not a good practice to use a large number of compensator in transmission link. Thus a number of compensator is first selected for even compensation then other parameters are determined for transmission over a desired distance.

The computed results also reveal that the performance of an optical CPFSK system is highly degraded due to the influence of self-phase-modulation (SPM) induced by GVD. The impact of SPM highly degrades the performance at larger input power level. The penalty corresponding to $BER=10^{-9}$ is 0.75dB when the power input to the fibre is $P_{in}=0\text{dBm}$ whereas the penalty is found to be 2.2 dBm when $P_{in}=8\text{dBm}$. It is found that penalty decreases with increase in compensator length and again increases after attaining a minimum penalty which corresponds to full dispersion compensation. At higher input power level, the minimum penalty corresponding to full GVD compensation occurs at a small value of the compensating fibre length. This is due to the fact that the effect of SPM opposes the effect of GVD and the effect of SPM is more dominant at higher input power. Thus after full compensation of GVD, effect of SPM increases more rapidly with compensator length. It is further observed that penalty increases less rapidly in case of $h=0.5$ than $h=1$.

When linecoding schemes are used, the performance of the system is improved to some extent. For example, the penalty for $h=0.5$ is 0.38dB for AMI encoded data, 0.4dB for MC encoded data and 0.8 dB for DM encoded data. The penalty for $h=1$ is 0.44dB, 0.58dB and 0.64dB respectively. From these values it is observed that AMI encoding system suffers minimum penalty.

4.2 Future Works

The present research work can be easily extended to evaluate the relative efficiency of the dispersion compensation schemes in wavelength division multiplexing (WDM) optical transmission system with cascaded EDFAs. The approach can further be extended to linecoded CPFSK system.

Further study can be made to determine the impact of SPM and GVD on the performance of IM/DD system with single channel as well as WDM transmission when dispersion compensation schemes are employed with NRZ and linecoded data pattern.

Further research in this respect can also be initiated considering WDM transmission with a fibre ring network architecture. The impact of SPM on the channel separation requirements, required optical bandwidth of Fabry-Perot filter (FPF) to reduce the effect of accumulated ASE of EDFAs and the maximum number of nodes and ring diameter in terms of the length of the fibre sections etc. needs further investigation.

References :

- [1] G. Prati, "Coherent Optical Communications and Photonic Switching", Proceedings of the Fourth Tirrenia International Workshop on Digital Communications , Tirrenia, Italy, September 19-23, 1989.

- [2] F. M. Knox, W. Forysiak and N. J. Doran, "10 Gbt/s Soliton Communication Systems over standard fiber at 1550 nm and the use of dispersion compensation", Journal of Lightwave Technology, vol.13, no.10, October 1995, pp. 1955-1962.

- [3] R. A. Linke and A. H. Granuck, "High-capacity coherent lightwave systems", Journal of Lightwave Tech., Vol.6, pp. 1750-1769, Nov. 1988.

- [4] B. L. Patel, E. M. Kimber, M. G. Taylor, A. N Robinson, I. Hardcastle, A. Hadjifotiou, S. J. Wilson, R. Keys and J. E. Righton, "High performance 10 Gb/s optical transmission system using Erbium-doped fibre amplifier", Electronic Letters vol. 27 no. 23, pp. 2179-2180, Nov. 1991.

- [5] G. Jacobsen, K. Emura, T. Ono and S. Yamazaki, "Requirements for LD FM characteristics in an optical CPFSK system", Journal of Lightwave Technology, vol. 9, 1991, pp. 1113-1123.

- [6] S. Kobayashi, Y. Yamamoto, M. Saito and T. Kimura, "Direct Frequency modulation in AlGaAs semiconductor lasers", IEEE Journal of Quantum Electron, vol. QE-18, no.4, 1982, pp. 582-595.

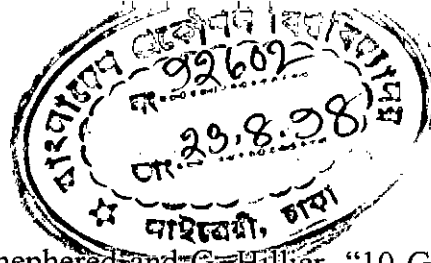
- [7] K. Iwashita and T. Matsumoto, "Modulation and detection characteristics of optical continuous phase FSK transmission system", *Journal of Lightwave Technology*, vol. LT-5, April 1987, pp. 452-260.
- [8] H. Toba, K. Oda, K. Nosu, N. Takato and H. Miyazawa, "5 GHz spaced eight channel optical FDM transmission experiment using guided wave tunable demultiplexer," *Electronic Letters*, vol. 24, 1988, pp. 78-80.
- [9] A.R. Chraplyvy, "Limitation of lightwave communication imposed by optical-fibre nonlinearities", *J. Lightwave Technology*, vol. 8, no. 10, October 1991, pp. 1548-1557.
- [10] D. Cotter, "Stimulated Brillouin scattering in mono mode optical fiber," *J. Optical Communications*, vol. 4, 1983, pp. 10-19.
- [11] "Effect of fibre nonlinearity on long distance transmission", *J. Lightwave Tech.* vol. 9, no. 1, pp. 121-128, Jan. 1991.
- [12] Robert G. Waarts, A. A. Friesem, "Nonlinear Effects in Coherent Multi-channel Transmission Through Optical Fibres" *Proceedings of the IEEE*, Vol. 78, No. 8, August 1996, pp. 1344-1367.
- [13] K. O. Hill, D. C. Johnson, B. S. Kawasaki and I. R. MacDonald, "CW three-wave mixing in single mode optical fibers," *J. Appl. Phy.*, vol. 49, 1978, pp. 5098-5106.
- [14] J.P. Hamaide, Ph. Emplit and J.M. Gabriagues, "Limitation in long haul IM/DD optical fibre systems caused by chromatic dispersion and nonlinear kerr effect", *Electron Lett.*, vol. 26, no. 18, pp. 1451-1453.

- [15] I. Garrett and G. Jacobsen, "Phase noise in weakly coherent systems," IEE proceedings- J. opto electronics, vol. 136, 1989, pp. 2179-2180.
- [16] I. Garrett, "Introduction to the effect of phase noise on coherent optical system," Proceedings of Forth Tirrenia International workshop on digital communication, Tirrenia, Italy, September 19-23, 1989, pp. 103-116.
- [17] A. F. Elrefaie and R. E. Wagner, "Chromatic dispersion limitations for FSK and DPSK systems with direct detection receivers," IEEE Photonics Technology Letters, vol. 8, no. 1, January 1991.
- [18] Md. Abdul Moqaddem, "Performance analysis of Direct Detection Optical FSK in the presence of Fibre Chromatic Dispersion", M.Sc. Engineering thesis submitted to the Dept. of Electrical and Electronic Engg., BUET, June 1996.
- [19] Md. Jahangir Alam, "Performance study of Optical Coherent and Direct Detection DPSK system in presence of Fibre Chromatic Dispersion", M.Sc. Engineering thesis submitted to the Dept. of Electrical and Electronic Engg., BUET, August 1996.
- [20] S.P.Majumder, R. Gangopdhyay and B.pal, " Sensitivity penalty for Direct Detection CPFSK due to laser phase noise and chromatic dispersion", J. Optical Commun., 1998(to appear).
- [21] D. J. Malyon and W. A. Stallard, "565 Mb/s FSK direct detection system operating with four cascaded photonic amplifiers," Electronics Letters, vol. 25, no. 8, 1989, pp. 495-496.

- [22] D. Marcuse, "Single-channel operation in very long nonlinear fibres with optical amplifiers at zero dispersion", *J. Lightwave Tech.* vol.8, no.10, pp.1548-1557, Oct. 1990.
- [23] M.J.O'Mahony, "Progress in optical amplifiers", *Proceedings of the Fourth Tirrenia International Workshop on Digital Communications*, Tirrenia, Italy, Sep.19-23, 1989, pp.73-84.
- [24] N.A. Olsson, "Lightwave systems with Optical Amplifiers", *Journal of Lightwave Technology*, vol.7, pp. 1071-1082, July 1989.
- [25] D.J. Malyon, T.Widdowson, E.G.Bryant, S.F.Carter, J.V. Wright and W.A. Stallard, "Demonstration of optical pulse propagation over 10000 km of fibre using recirculating loop", *Electron Lett.*, vol. 27, no. 2, pp. 120-121, 1991.
- [26] W. H. Loh, R. I. Laming, N. Robinson, F. Vaninetti, C. J. Anderson, M. N. Zervas, and M. J. Cole, "Dispersion Compensation Over Distances in excess of 500km for 10 Gb/s Systems Using Chirped Fiber Gratings", *IEEE Photonics Technol. Lett.* , vol. 8, no.7, 1996, pp 944-946.
- [27] N. Antoniadis, I. Roudas, R. E. Wagner, and S.F.Habiby, "Simulation of ASE noise accumulation in a wavelength add/drop Multiplexer Cascaded" *IEEE Photonics Technol. Lett.*, vol. 9, Sep. 1997.
- [28] Y.H.Cheng "Optimal design for direct detection system with optical Amplifiers and dispersion Compensators", *J.of Lightwave Tech.* ,Vol. 11, No. 9, September 1993 pp 1495-1499.

- [29] K. Takiguchi, K. Okamoto, and K. Moriwaki, "Planar Lightwave Circuit Dispersion Equalizer", *J. of Lightwave Tech.*, Vol. 14, No. 9, September 1996 pp 2003-2011. ✓
- [30] Akira Naka and Shaigeru Saito, "Transmission distance of In-Line Amplifier System with Group-Velocity-Dispersion Compensation", *J. of Lightwave Tech.*, Vol. 13, No. 5, May 1995, pp 862-867.
- [31] M. E. Marhic, N. Kagi, T. K. Chiang, and L. G. Kazovsky, "Optimizing the Location of Dispersion Compensators in Periodically Amplified Fiber Links in presence of Third-Order Nonlinear Effects", " *IEEE Photonics Technol. Lett.*, vol. 8, No. 1, 1996, pp.145-147.
- [32] S. Watanabe, and, M. Shirasaki, "Exact Compensation for both Chromatic Dispersion and Kerr effect in a Transmission Fiber Using Optical phase Conjugation " *J. of Lightwave Tech.*, Vol. 14, No. 3, March 1996, pp 243-248.
- [33] T. K. Chiang, N. Kagi, Michel E. Marhic, and L. G. Kazovsky, "Cross-Phase Modulation in Fiber Links with Multiple Optical amplifiers and Dispersion Compensators", *J. of Lightwave Tech.*, Vol. 14, No. 3, March 1996, pp 249-260.
- [34] R. J. Nuyts, Y. K. Park, and P. Gallion, "Dispersion Equalization of a 10 Gb/s Repeated Transmission System Using Dispersion Compensating Fibers", " *J. of Lightwave Tech.*, Vol. 15, No. 1, January 1997, pp 31-42.
- [35] N. Kikuchi and S. Sasaki "Analytical Evaluation Technology of Self-Phase-Modulation Effect on the Performance of Cascaded Optical

868-878, May 1995.



- [36] C. Rolland, R. S. Moore, F. Shepherds and G. Hillier, "10 Gb/s. 1560 nm multi quantum well InP/InGaAsP Mach-Zender optical modulator", Electronic Letters, vol. 29, no.5, March 1993, pp. 471-472.
- [37] N. Takato, T. Kominato, A. Sugita, K. Jinguji, H. Toba and M. Kawachi "Silica- Based Integrated Optic Mach-Zender Multi/Demultiplexer Family with Channel Spacing of 0.01-250 nm", IEEE Journal on Selected areas in Communications Vol. 8 No. 6, August 1990.
- [38] E. Bedrosian and S.O. Rice, "Distorsion and crosstalk of linearly filtered, angle-modulated signals", Proc. IEEE, vol.56, pp. 2-13, 1968.
- [39] R. Gangopadhyay, S. P. Majumder , P. Cochrane and E. Forestieri "Performance Analysis of a Direct Detection Receiver for AMI coded CPFSK Signals", IEEE Photon. Technol. Lett., vol.7, pp. 552-554, May 1995.
- [40] S. P. Majumder, R. Gangopadhyay, and G. Prati, "Effect of line coding on heterodyne FSK optical systems with nonuniform laser FM response", IEE Proc. -Optoelectron., Vol. 141, No. 3, June 1994, pp 200-208.
- [41] J. Wang, K Peterman, "Small signal analysis for dispersive optical fibre communication system", IEEE Journal of Lightwave Technology, 1992, No. 10, pp 96-100.